AD-A163 012 EVALUATION OF NOGAPS 21 (NAVY OPERATIONAL GLOBAL ATMOSPHERIC PREDICTION S.. (U) NAVAL POSTGRADUATE SCHOOL MONTEREY CA J S BOYLE ET AL. NOV 85 NPS63-85-002 1/1

UNCLASSIFIED F/G 4/2 NL

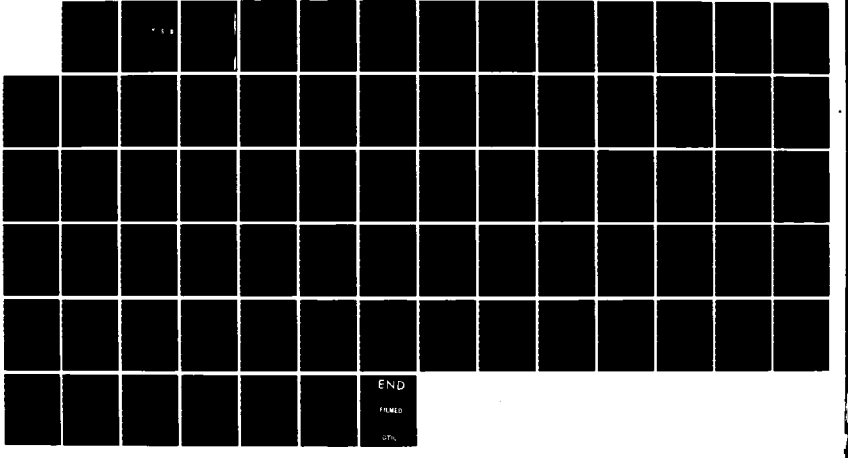

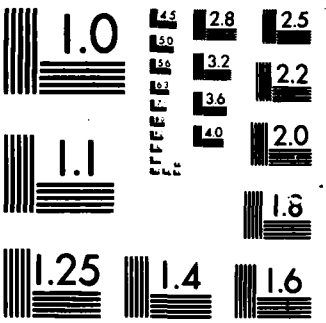

(2)

NPS63-85-002

NAVAL POSTGRADUATE SCHOOL

Monterey, California

Evaluation of NOGAPS 2.1

Systematic Error - Winter 1983/84

by

James S. Boyle and Carlyle H. Wash

November 1985

Technical Report

Approved for public release; distribution unlimited

Prepared for: Naval Environmental Prediction Research Facility
Monterey, California 93943

Naval Postgraduate School
Monterey, California

Rear Admiral Robert H. Shumaker
Superintendent

David A. Schrady
Provost

The work reported herein was supported in part by the NEPRF. Reproduction of all or part of the report is authorized.

This report was prepared by:

James S. Boyle
Adjunct Professor of Meteorology

Carlyle H. Wash
Professor of Meteorology

Reviewed by:

R. J. Renard, Chairman
Department of Meteorology

Released by:

J.N. Dyer
Dean of Science and Engineering

UNCLASSIFIED

SECURITY CLASSIFICATION OF THIS PAGE (When Data Entered)

REPORT DOCUMENTATION PAGE	READ INSTRUCTIONS BEFORE COMPLETING FORM
1. REPORT NUMBER: NPS63-85-002	2. GOVT ACCESSION NO.: AD-A163 812
	3. RECIPIENT'S CATALOG NUMBER:
4. TITLE (and Subtitle): Evaluation of NOGAPS 2.1 Systematic Error - Winter 1983/84	5. TYPE OF REPORT & PERIOD COVERED: Technical Report
	6. PERFORMING ORG. REPORT NUMBER:
7. AUTHOR(s): James S. Boyle and Carlyle H. Wash	8. CONTRACT OR GRANT NUMBER(s):
9. PERFORMING ORGANIZATION NAME AND ADDRESS: Naval Postgraduate School, Monterey, California 93943-5100	10. PROGRAM ELEMENT, PROJECT, TASK AREA & WORK UNIT NUMBERS: 62759N; WF59-553 N6685685WR5008
11. CONTROLLING OFFICE NAME AND ADDRESS: Naval Environmental Prediction Research Facility, Monterey, California 93943	12. REPORT DATE: November 1985
	13. NUMBER OF PAGES: 67
14. MONITORING AGENCY NAME & ADDRESS(if different from Controlling Office)	15. SECURITY CLASS. (of this report): Unclassified
	15a. DECLASSIFICATION/DOWNGRADING SCHEDULE:

16. DISTRIBUTION STATEMENT (of this Report)

Approved for public release; distribution unlimited.

17. DISTRIBUTION STATEMENT (of the abstract entered in Block 20, if different from Report)

18. SUPPLEMENTARY NOTES

19. KEY WORDS (Continue on reverse side if necessary and identify by block number)

systematic forecast error

numerical weather forecasts

20. ABSTRACT (Continue on reverse side if necessary and identify by block number)

This report presents an evaluation of the systematic error of the Navy Operational Global Atmospheric Prediction System (NOGAPS 2.1 for the winter of 1983/84. The systematic error is just the mean of the forecast error. The error is the difference between the NOGAPS forecast and the NOGAPS analysis at verification time. The fields examined are the 925, 500 and 250 mb heights. the 925 and 250 mb

DD FORM 1 JAN 73 1473 EDITION OF 1 NOV 65 IS OBSOLETE S/N 0102-014-6601

UNCLASSIFIED

SECURITY CLASSIFICATION OF THIS PAGE (When Data Entered)

winds, the 925-500 mb thickness and sea-level pressure. The forecasts are those started on the 0000 GMT watch for 120 h and are evaluated at intervals of 24 hours. The error and analysis fields are also Fourier decomposed along latitude circles to ascertain the scale structure of the errors.

In addition, anomaly correlations and root mean square error are computed over various latitude bands to provide an overview of the model performance.

Keywords: Numerical weather forecasting; Error analysis.

Evaluation of NOGAPS 2.1

Systematic Error - Winter 1983/84

James. S. Boyle

and

Carlyle H. Wash

6 November 1985

ABSTRACT

This report presents an evaluation of the systematic error of the Navy Operational Global Atmospheric Prediction System (NOGAPS 2.1) for the winter of 1983/84. The systematic error is just the mean of the forecast error. The error is the difference between the NOGAPS forecast and the NOGAPS analysis at verification time. The fields examined are the 925, 500 and 250 mb heights, the 925 and 250 mb winds, the 925-500 mb thickness and sea-level pressure. The forecasts are those started on the 0000 GMT watch for 120 h and are evaluated at intervals of 24 hours. The error and analysis fields are also Fourier decomposed along latitude circles to ascertain the scale structure of the errors.

In addition, anomaly correlations and root mean square errors are computed over various latitude bands to provide an overview of the model performance.

1. Introduction:

This is a summary report on the performance of the NOGAPS model for the winter of 1983/84. The results are presented chiefly in terms of mean monthly charts of systematic error and by graphs of anomaly correlation. The discussion focuses on the month of January 1984 since NOGAPS 2.1 data for this month was the most complete of the winter months (winter = Dec, Jan, Feb . The data used were exclusively from the forecast started at 0000 GMT since these integrations extended to 120 h.

2. January 1984

a. 500 mb Heights

Fig. 1A is a chart of the monthly mean 0000 GMT 500 mb NOGAPS analyses for January 1984. The pattern is fairly typical compared to longer term averages. The major anomaly for the month is the very strong flow in the North Atlantic due to a negative anomaly north of 50N and a positive anomaly south of this latitude. A secondary anomaly was strong ridging along 130W, the western edge of North America. The anomaly patterns for 700 mb are presented by Quiroz (1984).

Fig. 1B is the systematic error of the 24 h forecasts of the 500 mb geopotential for the 0000 GMT runs for January 1984. The systematic error is defined as:

$$Z_{sys} = \frac{\Sigma\ Z_{FCST} - Z_{OBS}}{N}$$

where:

Z_{OBS} = NOGAPS 0000 GMT analysis

Z_{FCST} = Forecast valid at the observation time

(-) = average over all the available forecast/observation pairs for a given forecast projection

N = number of. forecast/analysis pairs available for given forecast projection.

As expected, the 24 h NOGAPS forecasts are, in general, quite credible. There are obvious problems apparently associated with the high terrain of the Tibetan Plateau (TIP) and Greenland. There is a less prominent error in the regions of the Rockies and Alaskan Range. The pattern is similar to that of the NMC/ECMWF errors at 24 hours documented by Bettge (1983) (his Fig. 1) for the 1980/81 winter. Specifically, areas of agreement with Bettge's results are the prominent negative error over the TIP and to its east, and over the Alaskan Range. Magnitude of this error pattern in all three models is comparable. Bettge attributes this error to incorrectly handled orographic forcing. There are notable differences in the 500 mb height errors in the subtropics. Bettge (1983) found distinct positive error centers over Indochina and the eastern North Pacific Ocean. In constrast, NOGAPS errors are positive but not major features of the pattern.

Fig. 1C is a chart of the northern hemisphere, 500 mb. geopotential systematic error for the 72 h forecast. Over a large part of the chart the 72 hour error represents a growth of the 24 h pattern, although the large error over the TIP has remained remarkably constant. There are large negative errors (forecast too low) over the TIP, Gulf of Alaska and Western Europe/North Atlantic, and large positive errors east of Japan and over eastern North America. There is a general tendency of positive error north of 60N with the exception of Greenland. The errors along the winter storm tracks (North Pacific, North Atlantic) have grown substantially as have the errors over the "cold poles" of Eastern Siberia and North Central Canada. These

positive polar errors are consistent with forecaster observations of upper-level flow which is excessively zonal and weak in longer range NOGAPS forecasts. In the exit region of the anomalously strong flow over the North Atlantic there is a substantial negative error centered at 55N, 20E over Northern Europe.

b. Thickness (925 to 500 mb)

Fig. 2A is the mean, monthly, 925-500 mb thickness for the 0000 GMT analyses for January 1984 and Fig. 2B is the systematic error of this quantity for the 72 h forecasts. Negative values (positive values) indicate regions where the forecast is too cold (warm). A 15 m error in this thickness is equivalent to a 0.85 K error in the column mean temperature. Prominent negative regions are the North Atlantic and western North Pacific Ocean. The forecast is too warm over Japan, eastern North America and Eastern Siberia. Eastern North America is anomalously cold for this month (Quiroz, 1984) but Eastern Siberia is anomalously warm. Comparing Figs. 2A and 2B there is a tendency for the model to be too warm in the regions of the Eastern Siberian and Canadian "cold poles."

Fig. 2C is a Fourier decomposition of the data from Fig. 2B, retaining just the planetary scale waves, zonal wave numbers 1, 2 and 3. This is presented in an attempt to isolate any problems forced by land/sea heating contrasts which in the Northern Hemisphere probably force this scale. Broadly speaking, Fig. 2C shows that north of 30N the eastern oceanic basins are too cold and the eastern continental regions are too warm. A similar error pattern was documented for the earlier NMC PE model by Wallace and Woessner (1981). The warm pocket thrusting east of Japan contrasts with the errors along eastern North America which parallel the coastline. The polar regions north of 60N are everywhere too warm.

c. Sea-Level Pressure

Fig. 3A is the monthly mean sea-level pressure for the January 1984 0000 GMT analyses. Fig. 3B is the 72 h systematic forecast error of sea-level pressure. The lows in the Gulf of Alaska and over Iceland are forecast too low, while the ridging off the southeast Asia coast is underforecast. The large negative error pattern in the North Pacific and North Atlantic Oceans is likely associated with the NOGAPS tendency not to fill mature lows fast enough. Also, FNOC meteorologists have noted that NOGAPS will forecast North Pacific Ocean mature lows to move inland erroneously. The large negative error over Alaska is associated with this tendency. NOGAPS has a tendency to move continental highs offshore in east Asia too slow. This error is likely coupled to the underforecast of ridging over the Asian coast. There is a major negative forecast error center over Europe under the 500 mb diffluent region. This low SLP forecast compensates the low 500 mb forecast and results in a small thickness error in this region. There are relatively small sea level pressure errors in the polar regions. Almost the entire Asian continent north of 30N displays a negative error.

d. Wind Fields 250 and 925 mb

Fig. 4A is the monthly mean 925 mb wind field and Fig. 4B is the systematic error of the field at 72 hours. The scale of the wind vectors are in the upper right-hand corner of the plot. The number corresponds to the speed to which a vector of 10° longitude in length corresponds. All the vector lengths are scaled accordingly. Thus, if the scale is 80 ms^{-1}, then a vector representing 40 ms^{-1} would be 5° of longitude in length. The error field shows coherent circulation patterns which hopefully will facilitate identification and correction of error sources upon further analysis. The

error pattern is in approximate geostrophic balance with the sea-level pressure error of Fig. 3B.

There appear to be circulation errors along the equator in the regions of the mean convection centers, Indonesia, Brazil and equatorial Africa. The Australian monsoon flow onto the continent is somewhat underforecast as it is in South America and Africa. The northeasterly monsoon flow off the southeast Asian land mass is also a region of prominent error. The strong southerly flow indicated just south of Japan in Fig. 4B is consistent with (and perhaps an underlying cause of) the warm error in the thickness field. Similarly, the southerly flow over Hudson's Bay in Fig. 4B is also associated with cool thickness errors. Both may be an indication of model failure to develop cold polar anticyclones. An anticyclonic-error circulation is centered in northern Mexico, yielding strong southerly flow off the Baja coast. There are erroneously strong westerlies from Spain eastward into Asia.

Fig. 5A is the monthly mean 200 mb wind analysis for January 1981, and Fig. 5B is the 72 h systematic error. As in the lower-level wind fields, errors at 200 mb appear to be coherent circulation patterns in the error fields. Some of the most prominent errors occur over the oceanic regions where the data are sparse, thus it is difficult to assess the true error. However, at 250 mb and 925 mb also the use of satellite and aircraft reports make this level one with the most reliable wind analyses in oceanic regions.

In midlatitudes there is an apparent relation between the site of errors and the axis and exit regions of the North America and east Asian jet maxima. There is a definite underforecast of the ridge on the North American coast with a cyclonic error circulation in the Gulf of Alaska. The circulation pattern of cyclonic error just over the southern Japanese Islands might be an indication that the jet maxima is forecast too far north.

In the tropics the Australian monsoon circulation is a region of prominent error with an anomalous anticyclonic circulation over the continent. The tropics have some large percentage errors relative to the mean flow. For example, the weak flow off the eastern South American coast near the equator is a region of error comparable to that of the midlatitude jet regions where the mean flow is quite small. The errors in the tropics are not restricted to the climatological convectively-active regions.

e. Hovmuller Plots 500 mb Geopotential

Fig. 6A is a time-longitude (Hovmuller) plot of the 0000 GMT analyzed 500 mb geopotential for January 1984. The values are averages over the latitude band from 30N to 60N. Fig. 6A presents the deviations of the height field from its zonal mean for the total field while Fig. 6B is the same field only for the zonal wave numbers 1, 2 and 3. In both charts the positions of the troughs (dashed lines) and ridges (solid) corresponding to Fig. 1A are quite clear.

Figs. 7A and 7B are the same plots as in Figs. 6A and 6B but for 96 h forecasts of NOGAPS. It should be made clear that this is not a continuous run of the model but represents 26, 96 h forecasts all starting from different initial conditions. NOGAPS did not run out to 96 hours on the 10th and 21st of the month and these data gaps were linearly interpolated. Given the discontinuous nature of these model runs, the smoothness of the diagrams gives evidence of the effectiveness of the data assimilation/forecast cycle. Comparing Figs. 6A and 7A and 6B and 7B one finds that the NOGAPS 96 h forecast is quite representative.

Figs. 8A and 8B are the differences (FORECAST - OBSERVED) between Figs. 7A and 6A and 7B and 6B. There does not appear to be any longitude which is blatantly in error for all forecasts. However, forecast problems

appear centerd near 150W and the Greenwich meridian in Fig. 8A, and 150W, 60W and Greenwich meridian in Fig. 8B. The 60W and 0E are areas where there is high variability in the pattern (i.e., alteration of high and low heights). The model seems fairly skillful in the region of the standing trough at 150E. Comparison of Fig. 8B with 8A indicates that there is significant error in the planetary scale waves.

A prominent blocking event occurred off the western North America coast in the Gulf of Alaska region during the period from 10 to 20 January 1984 (Quiroz, 1984). This blocking was manifested by a prominent, persistent ridge near 150W. This strong ridging is especially evident in the planetary wave diagram, Fig. 6B. Comparison between Figs. 6B and 7B shows this blocking ridge is evidently handled adequately by the NOGAPS model at 96 hours. There is evidence (Fig. 8B) of a model tendency to underforecast the ridge and perhaps be a little slow in its formation and decay; however, the essentials of this important feature are clear in the forecast.

The value of this chart (Figs. 8A,B) is to show that the systematic error patterns of the preceding figures are not the result of one or two catastrophic forecasts. The figures indicate that the systematic errors can be the result of a sometimes subtle error tendency which can be completely absent or reversed on any given single chart. The systematic errors can be masked by other developments and are not observed as a constant bias at any particular location.

Figs. 8A and 8B also suggest a closer analysis, with larger time series, of periods when the model performed poorly and when it performed well. There appears to be a tendency for errors to persist through a number of forecast/analysis cycles. It would be of value to determine if these errors

are "regime oriented", that is, are there particular flow patterns for which the model can be expected to perform poorly.

f. Anomaly Correlations .

Fig. 9 is a graph of anomaly correlation coefficient versus forecast projection for 500 mb heights, averaged over the latitude band from 30N to 60N for January 1984. The anomaly correlation coefficient (ACC) is defined as in Miyakoda et al. (1972):

$$ACC = \frac{\overline{\Delta x_f(\tau) \cdot x_o(\tau)}}{(\Delta x_f)^2 \quad (\Delta x_o)^2}$$

where: τ = forecast interval

$\Delta x(\tau)$ = $x(\tau) - x_c$: x_c = climatology

Δx_f = forecast anomaly for given τ

x_o = analysis anomaly

$(\overline{\ })$ = spatial average over all equally weighted grid points

$[\ ]$ = average over all the forecast/analysis pairs for the month.

The climatology used is the monthly mean field from the available NOGAPS 0000 GMT analyses. This differs from the common practice of using a longer term climatology but should not have a large impact on the actual values of the ACC. The ACC is computed for the Fourier analyzed fields. These spectral ACC's are divided into bands of zonal wavenumber 1 to 3, 4 to 7 and 8 to 12.

Fig. 9 clearly shows that the planetary scale waves achieve the best scores at all forecast projections, with their advantage growing slightly in time. A rule of thumb, generally accepted, is that a forecast still contains useful information if its ACC is above 0.6. Using this criterion, the planetary wave forecast (1, 2, 3 is useful in this latitude band out to

120 h. The shortest waves (8-12) fall below this value at 72 h. Fig. 9, compared to similar plots generated by NMC and ECMWF, indicates that NOGAPS is competitive to forecasts produced by these centers but generally its forecast deteriorates at a more rapid rate. NMC's planetary wave forecast ACC does not fall below 0.6 until day 7 for the January 1984 period, Ward (1984).

Fig. 10 is the same as Fig. 9 except that the data are for the latitude band 0 to 30N. In this band the planetary wave forecast loses its superiority, and the forecast deteriorates more rapidly than the midlatitude band of Fig. 9. All wave groups fall below 0.6 before day 3.

Fig. 11 is a time series of the ACC for the month of January 1984 for the midlatitude band (30N-60N) for 72 h forecast of 500 mb height. There are periods of good and bad forecasts as previously indicated by the Hovmuller diagrams. In general, the planetary scale waves are superior on a day-to-day basis, although there are a few periods where they fall from pre-eminence. There are some catastrophic synoptic scale wave forecasts, but the average monthly values give a good idea of the day-to-day performance. Generally, the forecast is reliable out to 72 h. It might be of some value to investigate and contrast the periods during which the model performs well and those which is does poorly. This is a topic of interest to the ECMWF Benedetti & Simmons, 1983 .

Fig. 12 is the same as Fig. 9 but for 925-500 mb thickness. This gives a measure of both the 500 and 925 forecast fields. As expected, there is a faster falloff in this figure than the 500 mb ACC since the errors of the 925 fields are added to the 500 mb error and evidently they are correlated.

g. Mean Thickness Error - January 1984

Fig. 13A is a plot of the mean error of the 925-500 mb thickness for the polar band (60N to 85N) for January 1984. The mean error is positive

(forecast too warm) and grows rapidly with time. On the average, by 120 h the 925-500 mb column is 4 K degrees too warm in the NOGAPS forecast. Fig. 13B is the same as Fig. 13A only for the midlatitude band (30N-60N). Again, the error is positive but only half that of the polar band at 120 h. The tropical band (0-30N) also shows a positive mean error, but only 1.1 K at 120 h. The model on a global average, and by bands, has a problem in becoming too warm in the lower troposphere. Calculations of the 925-250 mb thickness error indicate that the positive bias is true for this thickness also.

3. Systematic Errors - December 1983

Figs. 14 through 21 are the figures for December 1983 corresponding to Figs. 1 through 13 (January 1984). NOGAPS version 2.1 became operational on 8 December 1983 and the figures are the forecast data from 8 December 1983 through 31 December 1983.

Fig. 14A is the monthly mean 500 mb height for the 0000 GMT NOGAPS analyses for December 1983. A very prominent feature on the chart is the ridge centered in the Gulf of Alaska. This anomalous feature is the result of persistent blocking in the region for almost the entire December 1983 period Quiroz, 1984). The effect of this blocking ridge resulted in the U.S. experiencing one of the coldest Decembers on record Quiroz, 1984). Other large scale features of the 500 mb pattern, particularly pronounced by wave trough activity, over east Asia & eastern North America, are similar to January 1984.

The systematic 72 h error of 500 mb geopotential, Fig. 14B, indicates that this important, persistent pattern was handled satisfactorily by the model. However, the west coast of North America is, however, a site of some rather negative significant errors. Common error patterns between January 1984 and December 1983 include:

(i) positive error south and east of Japan (also in thickness),

(ii) positive errors over the polar region (also in thickness),

(iii) positive errors over eastern North America associated with the long wave trough,

(iv) negative error over Europe and eastern North Atlantic Ocean (with positive error couplet to the south) associated with diffluent flow.

Another aspect of these problems is revealed in Fig. 15B which is the 925-500 mb thickness systematic error for December 1983. The thickness is clearly too high over almost all of North America. The model is failing to fully capture the blocking-type flow that characterized the month and led to very cold air thrusting southward into the continent. A similar tendency on a lesser scale was observed in the January 1984 data.

The December 1984 SLP errors that are similar to those in January 1984 are

i) negative 8 to 12 mb errors over Asian continent and East Asian coast,

ii) negative 4 to 8 mb errors over Europe and east of Greenland associated with more vigorous cyclone activity,

iii) negative errors along the western North American coast. These errors are under the main belt of westerlies, suggesting that the erroneous movement of cyclones inland contributes to this error.

The remainder of the December 1983 figures will not be discussed in any detail for the sake of brevity. Most of the patterns speak for themselves: as more complete data sets are collected, a more thorough analyses will be undertaken.

4. Systematic Errors - February 1984

The data available for February 84 were limited to only half of the month (1 through 14 February 84). The flow pattern for February 84 presents an interesting contrast to December 1983, especially over North America. The strong Gulf of Alaska ridging (blocking) was replaced by anomalous troughing in the same position. A prominent ridge developed in western Asia centered at 50N, 50E. Fig. 22A is the February 84 monthly mean 500 mb heights from the 0000 GMT analyses (actually only using 1 - 14 February 1984 0000 GMT). The trough over Alaska and ridge at 50E are prominent features (compare to Fig. 14A, December 1983). Fig. 22B is the 72 h error for the 500 mb geopotential for February 1984. The error pattern is similar to Fig. 14A, December 1983, with a major difference being the large positive center at 47N, 60E (just north of the Aral Sea). This is just downstream of the site of the anomalously strong ridging for the month. Despite the very different upstream flow pattern, the error pattern over North America is surprisingly like that of December 1983 (Fig. 14B) and January 1984 (Fig. 1C). This suggests that the low heights over North America are a result of physics or boundary problems rather than dynamics.

Fig. 23A is the mean 925-500 mb thickness for February 84 and Fig. 23B is the 72 h systematic error in the field. Again, there is a great deal of similarity to the error pattern of December 1983 (Fig. 15B). This similarity is apparent over North America despite the very different thermal character of the fields over North America for these two months (Quiroz, 1984).

Fig. 23C is the same data as in Fig. 23A but Fourier decomposed and retaining only the planetary scale zonal wave numbers (1, 2, 3). The pattern can be generalized by saying that the eastern and southern ocean basins are too cold, the southern and east coast of continents are too warm and

everywhere north of 60N is too warm. The region of anomalous ridging in western Asia is a center of warm bias.

The similarity of the patterns, of the planetary scale 72 h error if the 925-500 mb thickness, for the three months (Dec, Jan, Feb) points to a problem in the model related to geographical forcing rather than a "regime" type error. The flow regimes for these months (e.g., December 1983 and February 1984) were very different, yet the error patterns were similar.

5. NOGAPS 2.0 - Systematic Error - November 1983

An enlightening exercise is to look at data from the November 1983 NOGAPS forecasts which were run using NOGAPS version 2.0. Fig. 25A is the 925-500 mb thickness for the month of November 1983 and Fig. 25B is the 72 h forecast error. Contrasting the error pattern of Fig. 25B to Fig. 15B (December 1983, NOGAPS 2.1) the most prominent difference is over and to the east of the North American continent. In these regions the sign of the error is reversed. The error sign is also reversed in the northern half of the Asian continent but the magnitude of the error is relatively small. The warm center south of Japan is a feature common to both figures.

Figs. 15C and 25C depict the planetary wave error in the 72 h, 925-500 mb thickness field. November 1983 (Fig. 25C) has a tendency for the land to be too cold and the water too warm while December 1983 has the reverse features. A quantitive comparison is hampered by the fact that the forcing of the two months is different and in December the polar night has begun north of the Arctic circle. But perhaps we can make some tentative conclusions about the nature of the NOGAPS error on the 925-500 mb thickness.

An obvious first conclusion is that the NOGAPS 2.1 PBL heat transfer changed the way the atmosphere gained energy and perhaps the correction overshot the proper value. It appears that the new version has altered the

air/sea, land/sea heat exchange, yet the prominent positive error south of Japan is common to both months. This might indicate that this error is not due to the improper handling of the air/sea fluxes over the Kuroshio but perhaps a downstream effect of improper inclusion of the TIP effects.

The warm continents, especially in December and January, might be due to incorrect calculation of the radiative transfer. A similar conclusion was reached by Wallace and Woessner (1981) when they observed a similar error in the NMC PE model.

6. Summary and Conclusions

An investigation of forecasts errors by the Navy Operational Global Analysis and Prediction System (NOGAPS) has been presented. NOGAPS became operational in late 1981 with forecasts from an improved nine layer version commencing December 1983. The current verification study uses data primarily from the updated version and focuses on winter 1983-84 forecasts of up to 5 days.

A variety of forecast verification statistics have been examined for the three winter months. Anomaly correlations for NOGAPS 500 mb geopotential show similar characteristics to ECMWF and NMC results with planetary wave forecasts showing the most skill in midlatitudes. Monthly systematic error analyses have been prepared for 500 mb height, 1000-500 mb thickness, sea level pressure and 925 and 250 mb wind fields. Hovmuller diagrams of forecast error show the temporal distribution of errors which comprise the monthly systematic error. Nonsystematic error (Wallace & Woessner, 1981) also has been computed for the same variables.

Preliminary analysis reveals repeatible systematic height errors associated with the elevated terrain of the Tibetan Plateau, Rocky Mountains and Greenland. Systematic thickness errors indicate the forecast atmosphere

is too cold over warm oceanic currents. Large errors in the 925 mb wind fields have been isolated near the southern tip of Greenland and over the South China Sea in the region of northeast monsoon. Future efforts will be directed toward studying the 1984 summer model errors. Whenever possible, NOGAPS error structures will be compared to verification results of other global prediction systems.

REFERENCES

Bengtsson, L. and A. J. Simmons, 1983: Medium-range weather prediction operational experience at ECMWF. Large-Scale Dynamical Processes in the Atmosphere. Ed. B. Hoskins and R. Pearce, Academic Press, New York, 397 pp.

Bettge, T. W., 1983: A systematic error comparision between the ECMWF and NMC prediction models. Mon. Wea. Rev., 111, 2385-2389.

Miyakoda, K., G. D. Hembree, R. F. Strickler and I. Shulman, 1972: Cumulative results of extended forecast experiment: I. Model performance for winter cases. Mon. Wea. Rev., 100, 836-855.

Quiroz, R. S., 1984: The climate of the 1983-84 winter - a season of [illegible] blocking and severe cold in North America. Mon. Wea. Rev., 112, [illegible] 1912.

Wallace, J. M. and J. K. Woessner, 1981: An analysis of forecast error in the NMC hemispheric primitive equation model. Mon. Wea. Rev., 109, 2141-2149.

Ward, J. H., 1984: NMC Monthly Performance Summary. Vol. 1, No. 1. National Meteorological Center, Washington, DC 20233.

LIST OF FIGURES

6A Time versus longitude plot (Hovmuller diagram) for the 500 mb geopotential for Jan 1984. The data plotted are average values for the latitude band from 30N to 60N. The contour interval is 60 m.

6B As in Fig. 6A except for the planetary scale waves, zonal wave numbers 1 to 3. Contour interval is 60 m.

7A As in 6A except for the Tau = 96 forecasts. Contour interval is 60 m.

7B As in 6B except for the Tau = 96 forecasts. Contour interval is 60 m.

8A As in 6A except for the Tau = 96 forecast error (FORECAST - OBSERVED). Contour interval is 60 m.

8B As in 6B except for the Tau = 96 h forecast error. Contour interval is 30 m.

9 Average anomaly correlation for 500 mb geopotential for a latitude band from 30N to 60N for Jan 1984 for forecast projections out to 120 hs. The ⊠ = planetary waves (1, 2, and 3), ● = total, * = long waves 4, 5, 6, and 7) and ⊕ = synoptic waves (8 to 15).

10 As in Fig. 9 but for the latitude band 30N to the equator.

11 Anomaly correlation for 72 h forecasts for the month of Jan 1984 for the 500 mb geopotential average over the latitude band 30N to 60N. The values on the extreme right hand side (day = 32) are the monthly means seen in Fig. 9. ⊠ = planetary waves, ● = total, * = long waves and ⊕ = synoptic scale waves.

12. As in Fig. 9 but for the 925-500 mb thickness.

13A Mean error for the 925-500 mb thickness for the latitude band 60N to 85N for Jan 1984.

13B As in Fig. 13A except for the latitude band 60N to 30N.

13C As in Fig. 13B except for the latitude band 30N to equator.

14A As in Fig. 1A except Dec 1983. Contour interval is 60 m.

14B As in Fig. 1C except Dec 1983. Contour interval is 15 m.

15A As in Fig. 2A except Dec 1983. Contour interval is 60 m.

15B As in Fig. 2B except Dec 1983. Contour interval is 15 m.

15C As in Fig. 2C except Dec 1983. Contour interval is 10 m.

16A As in Fig. 3A except Dec 1983. Contour interval is 4 mb.

16B As in Fig. 3B except Dec 1983. Contour interval is 2 mb.

17A As in Fig. 4A except Dec 1983.

17B As in Fig. 4B except Dec 1983.

18A As in Fig. 5A except Dec 1983.

18B As in Fig. 5B except Dec 1983.

19 As in Fig. 9 but for Dec 1983.

20 As in Fig. 12 but for Dec 1983.

21 As in Fig. 13A but for Dec 1983.

22A As in Fig. 1A but for Feb 1984. Contour interval is 60 m.

22B As in Fig. 1C but for Feb 1984. Contour interval is 30 m.

23A As in Fig. 2A but for Feb 1984. Contour interval is 60 m.

23B As in Fig. 2B but for Feb 1984. Contour interval is 15 m.

23C As in Fig. 2C but for Feb 1984. Contour interval is 15 m.

24A As in Fig. 3A but for Feb 1984. Contour interval is 4 mb.

24B As in Fig. 3B but for Feb 1984. Contour interval is 2 mb.

25A As in Fig. 2A but for Nov 1983. Contour interval is 60 m.

25B As in Fig. 2B but for Nov 1983. Contour interval is 15 m.

25C As in Fig. 2C but for Nov 1983. Contour interval is 5 m.

26A As in Fig. 3A but for Nov 1983. Contour interval is 4 mb.

26B As in Fig. 3B but for Nov 1983. Contour interval is 2 mb.

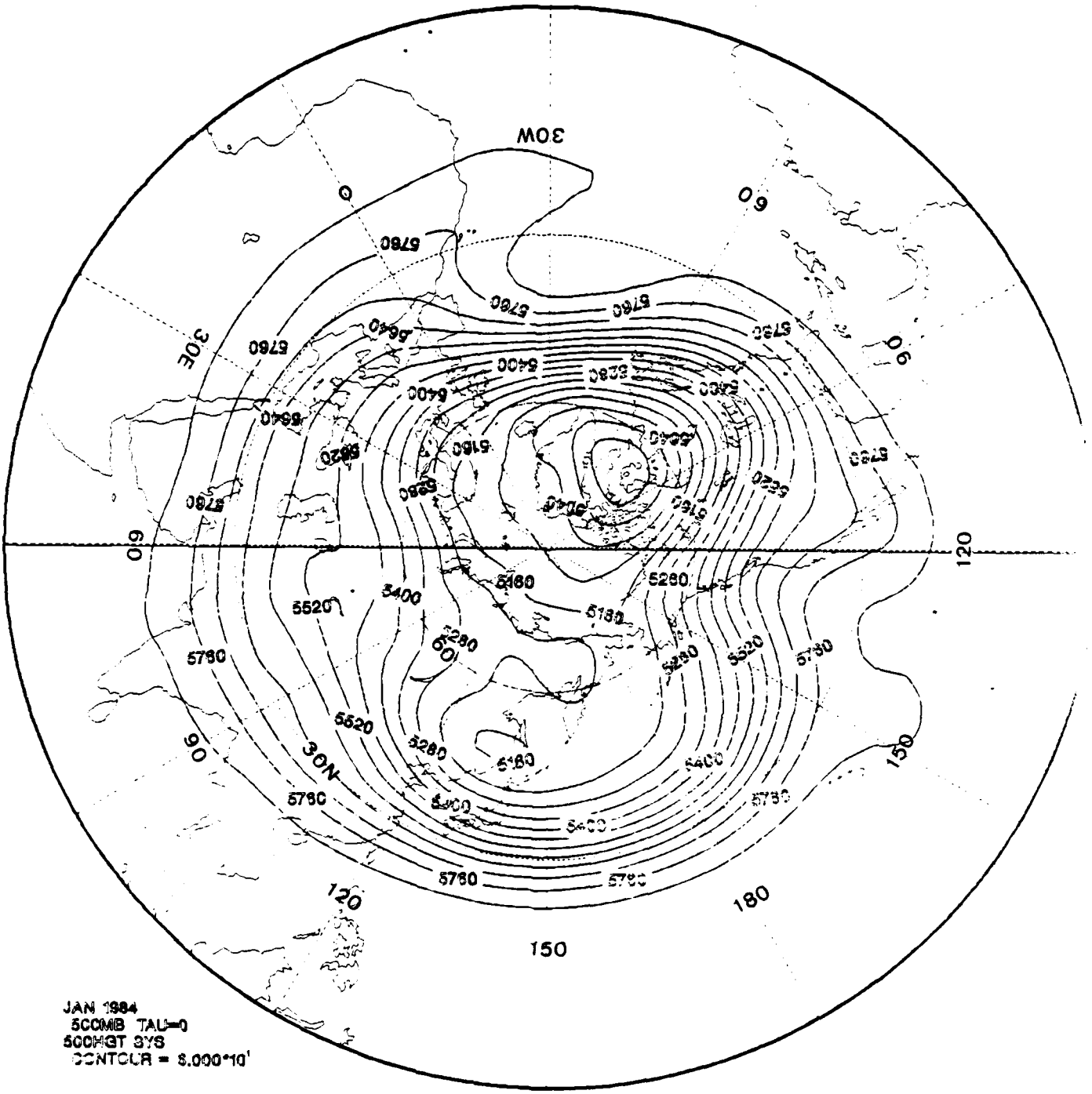

A Northern mean 500 mb geopotential analysis for Jan 1984. [illegible] mean were the 0000 GMT NOGAPS analyses. Contour interval is 60 m.

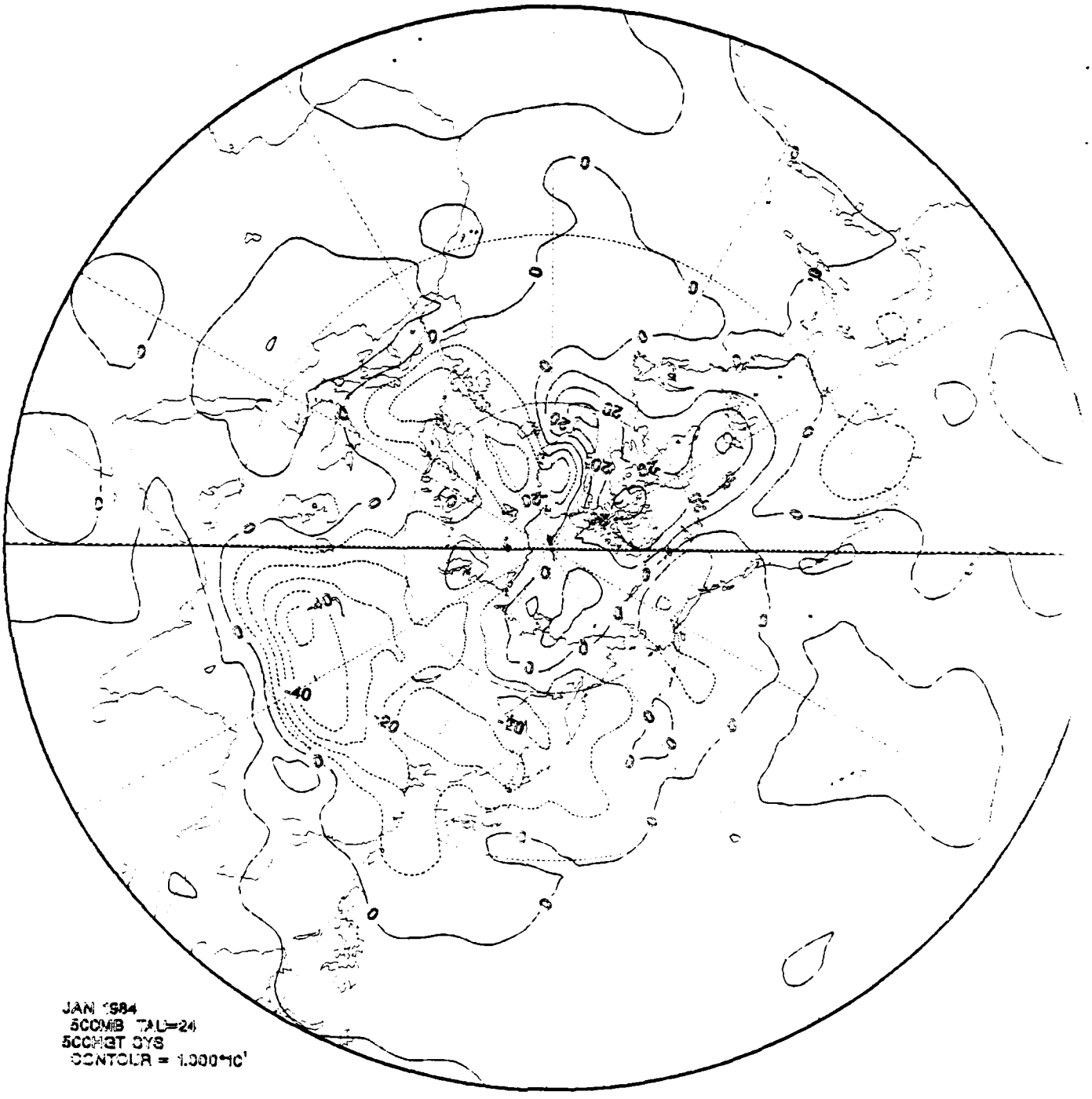

...matic error for 500 mb geopotential for ... Contour interval is 10 m. Dashed lines indicate negative ... lines indicate positive errors.

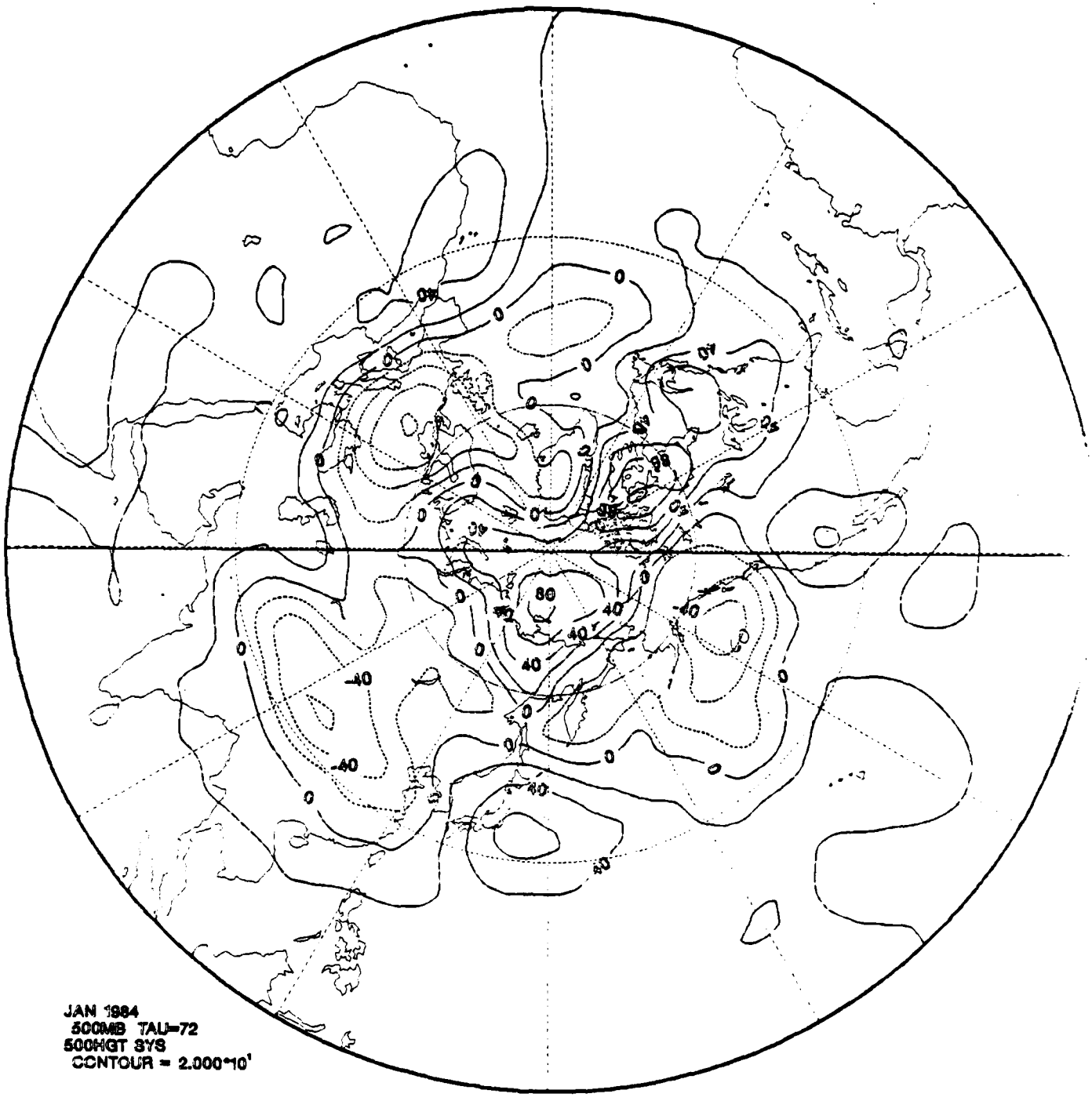

as in 1B except for Tau = 72 hours. Contour interval is 20 m.

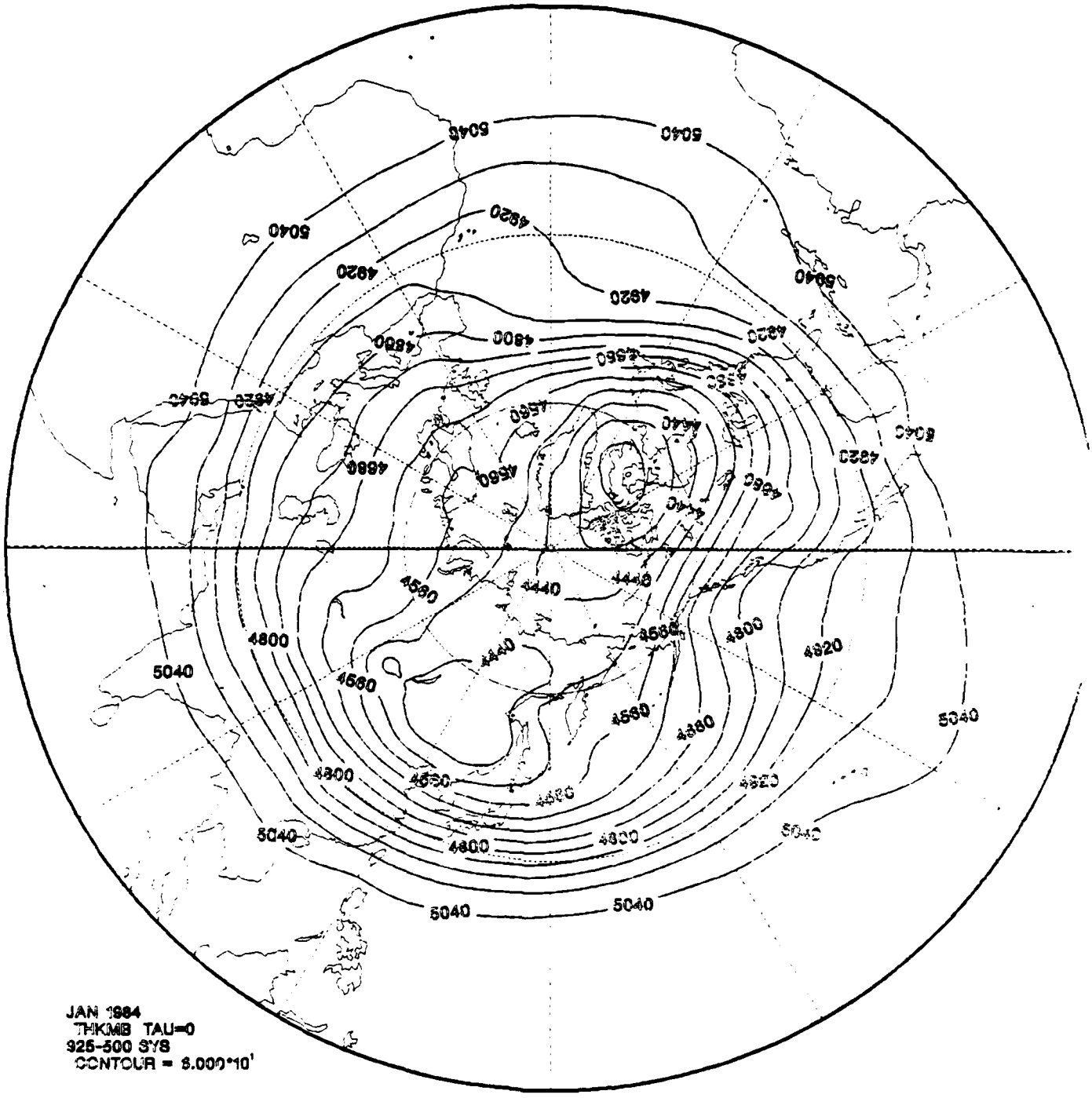

a. Monthly mean 925-500 mb thickness analysis for Jan 1984. All the mean were the 0000 GMT NOGAPS analyses. Contour interval is 60 m.

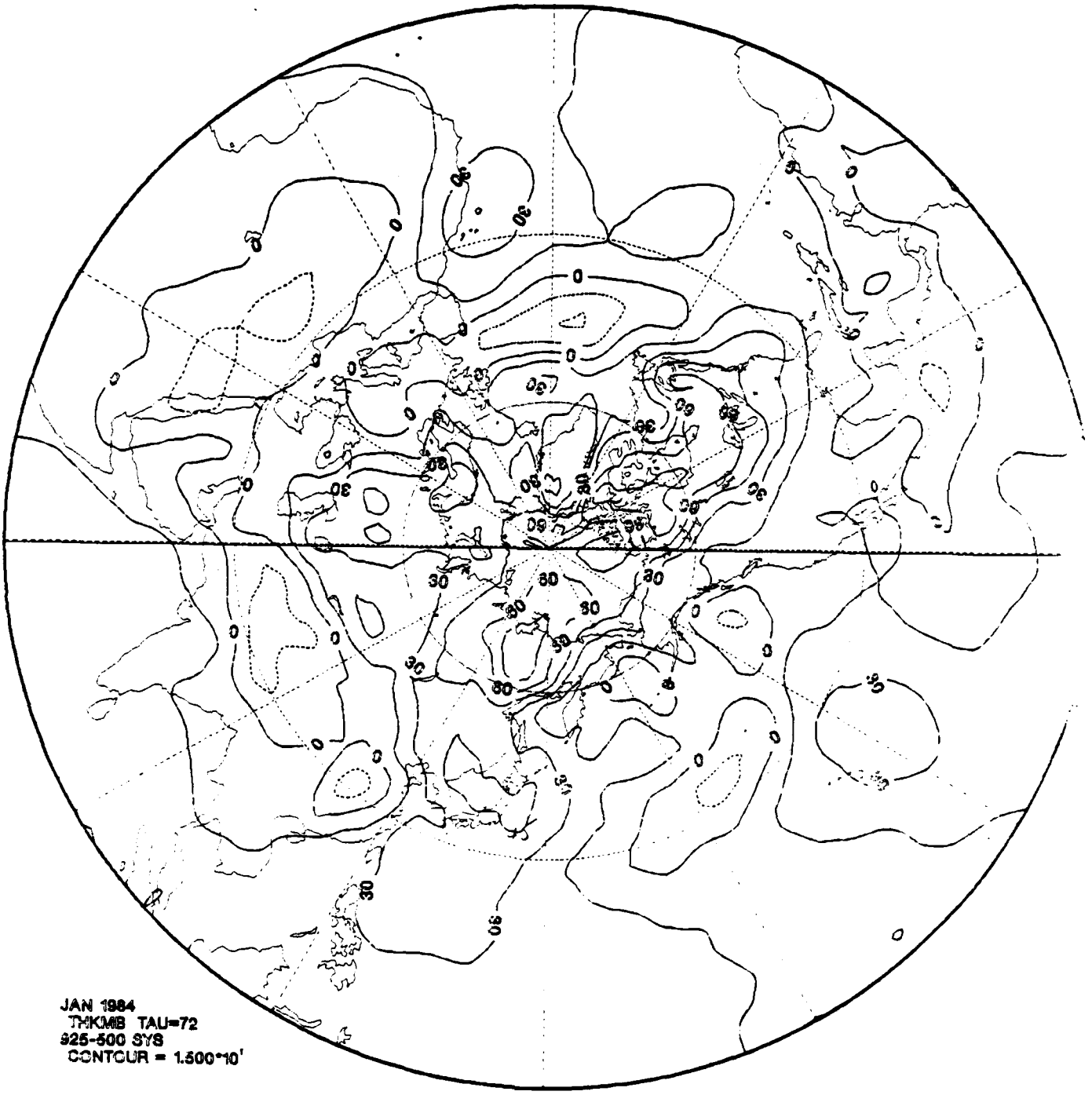

...systematic error for 925-500 mb thickness for Jan 1984. ...
Contour interval is 15 m. Dashed lines indicate negative values. ...
lines indicate positive values.

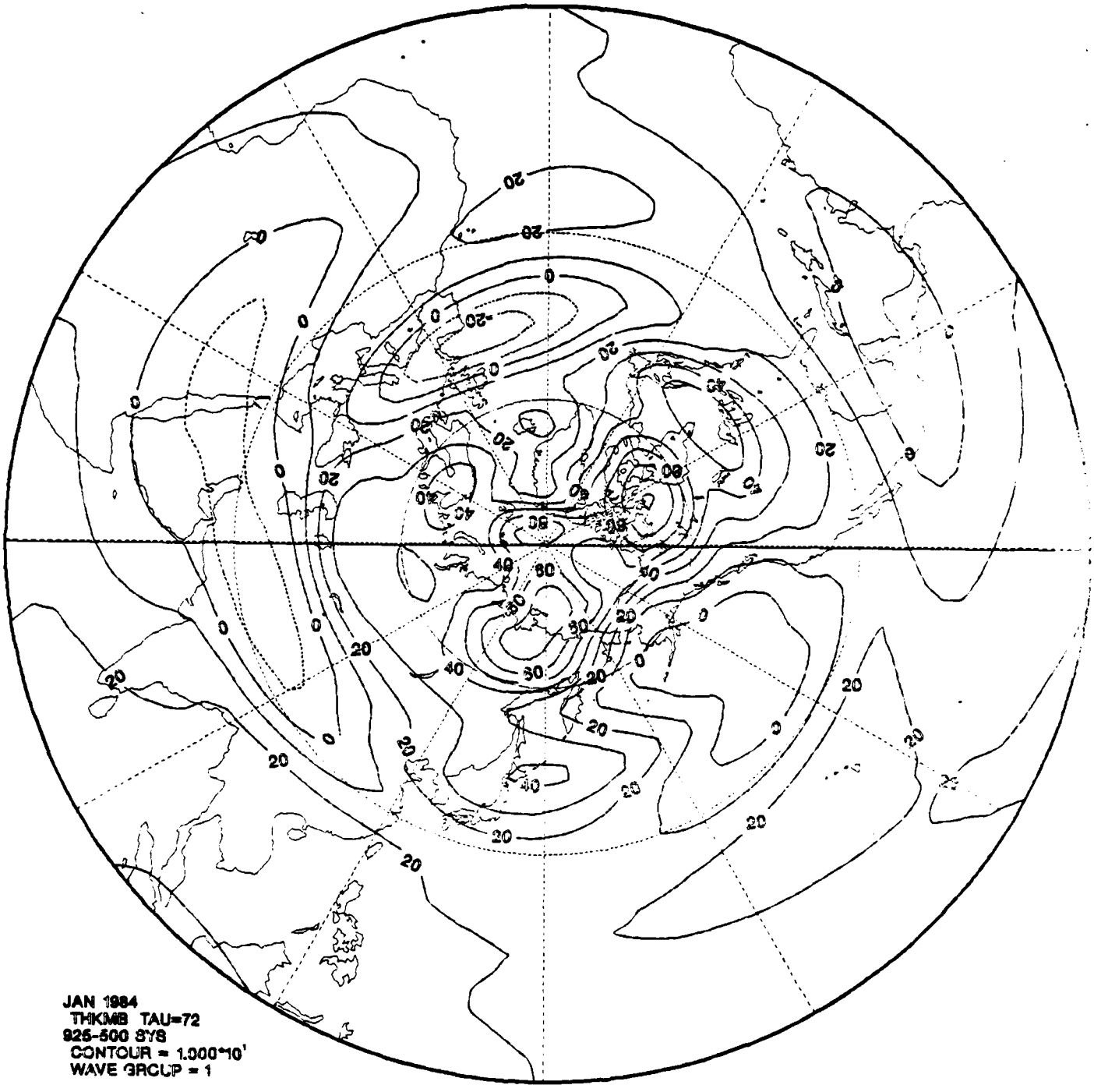

Planetary scale systematic error for 925-500 mb thickness for [illegible] Fourier decomposition of the data from [illegible] zonal wavenumbers 1 to 3. Contour interval is 10 m. Dashed lines are negative values, solid lines are positive values.

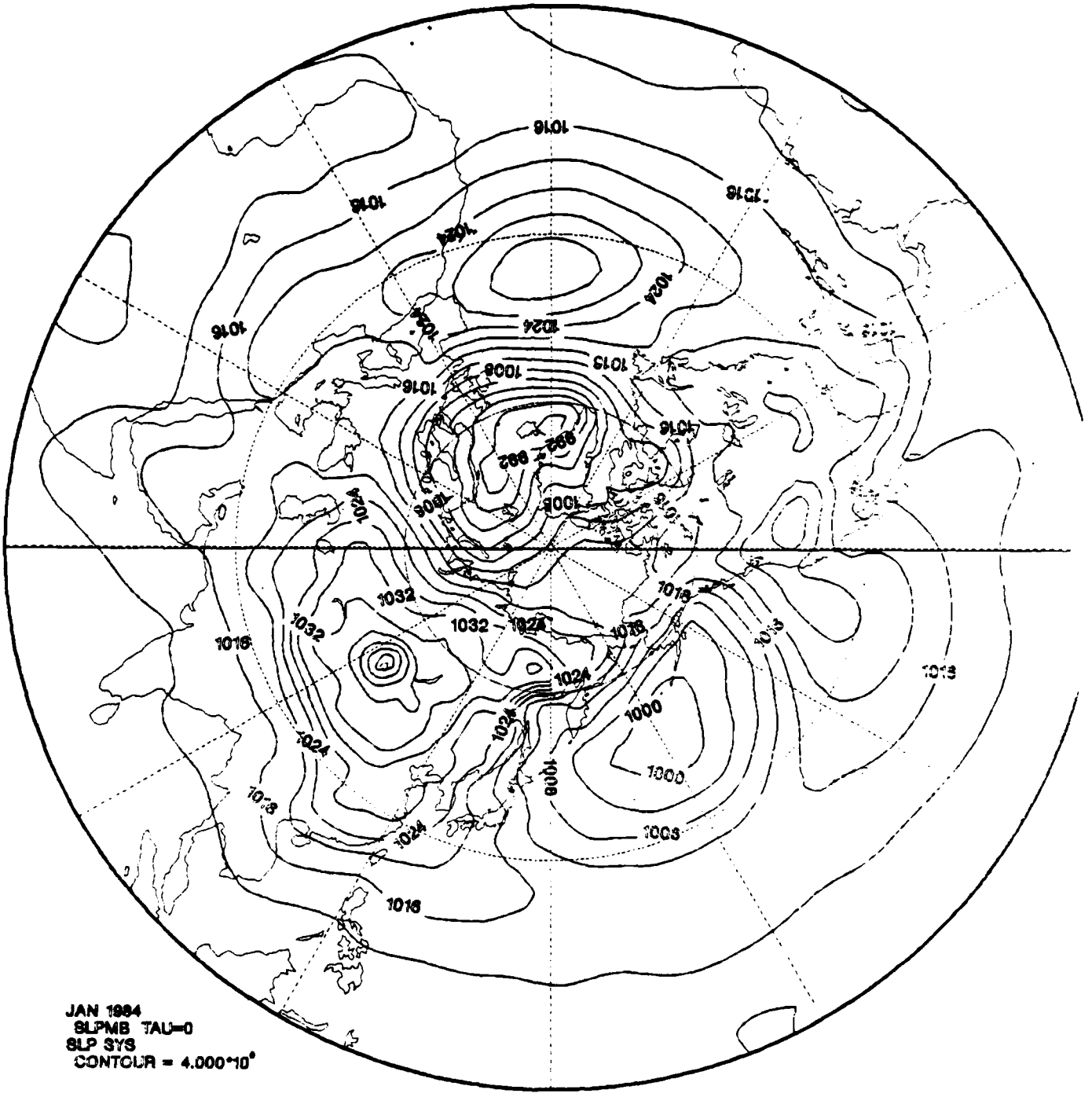

As in Fig. 1A except for sea-level pressure. Contour interval is 4 mb.

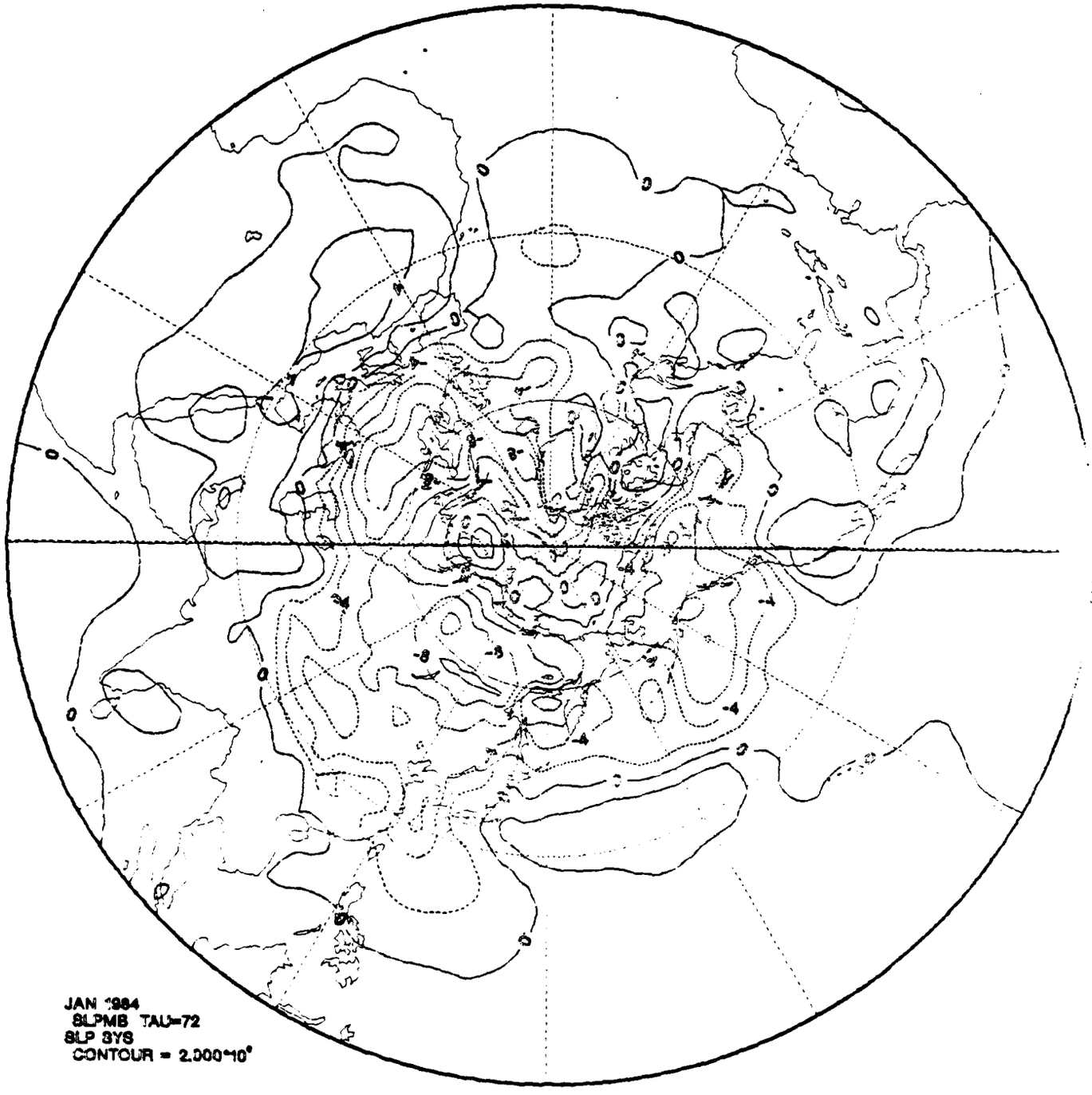

as in Fig. 6 except for sea-level pressure. Contour [illegible]

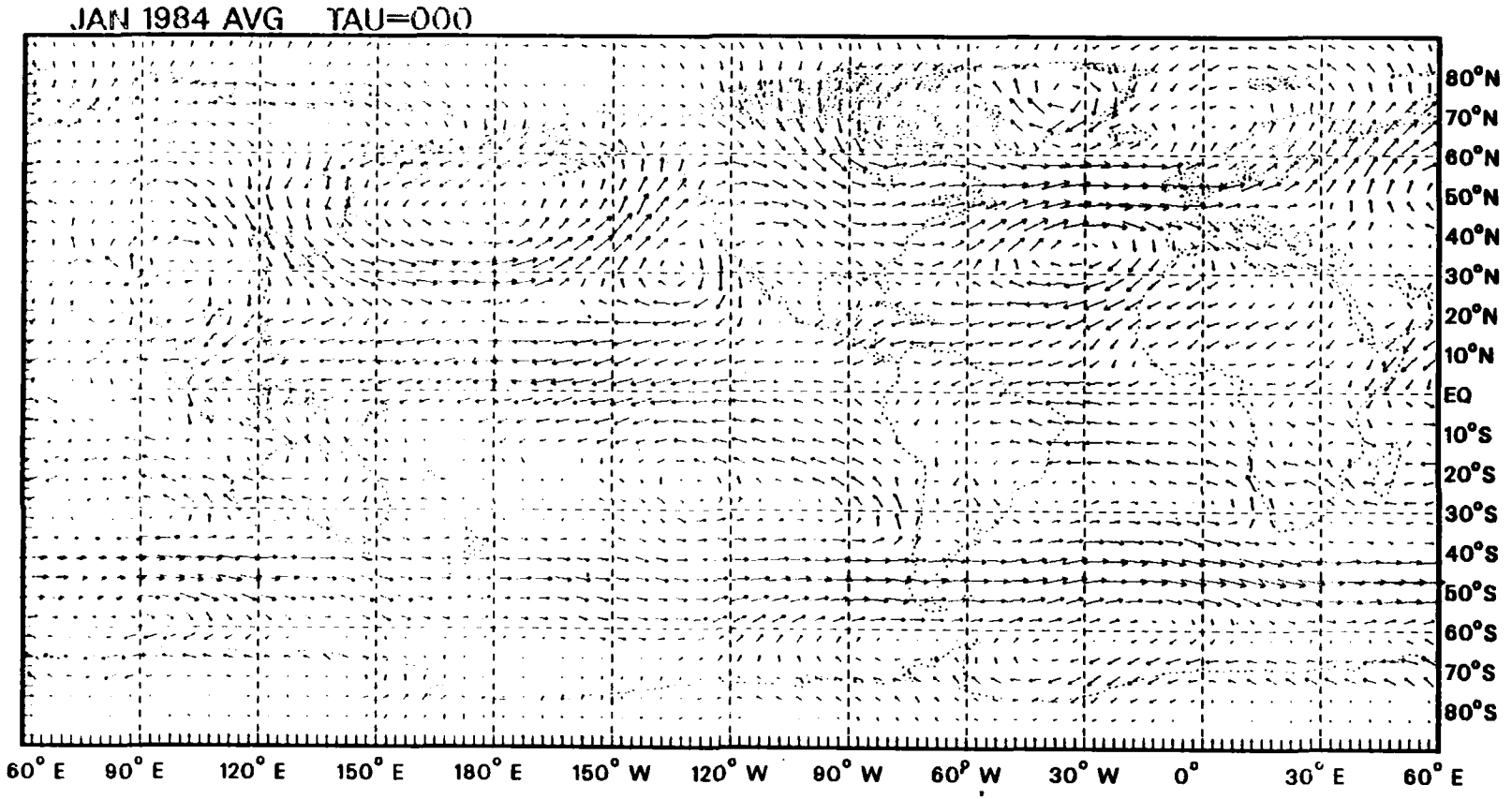

1A Monthly mean 850 mb wind field for Jan 1984. Data for the mean were the 0000 GMT Nogaps analyses. Scale for the wind vector is on the upper right hand corner of the figure.

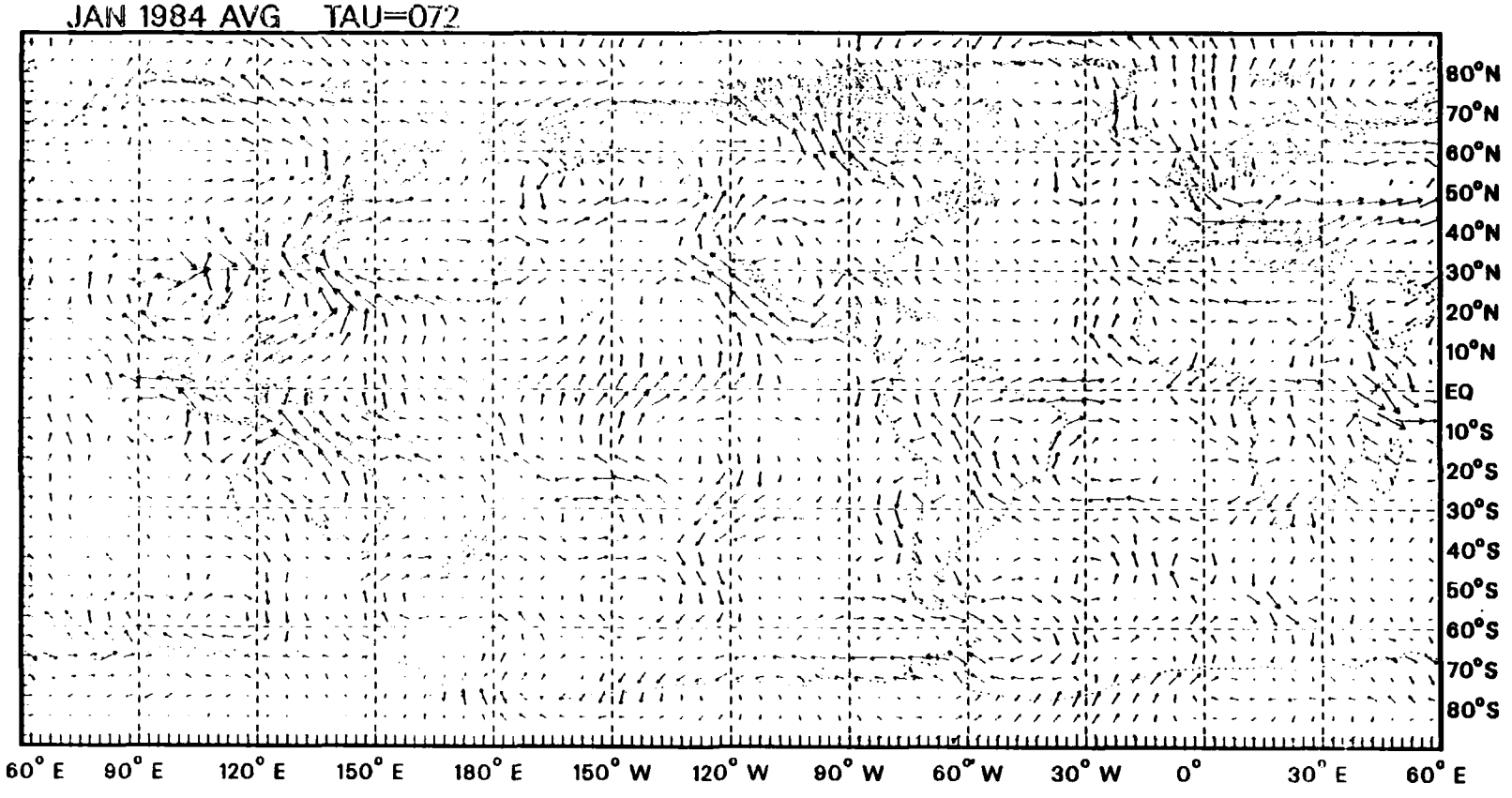

IB Systematic error for the 925 mb wind for Jan 1984 for Tau 72 hrs.

Scale for the wind vector is on the upper right corner of the figure.

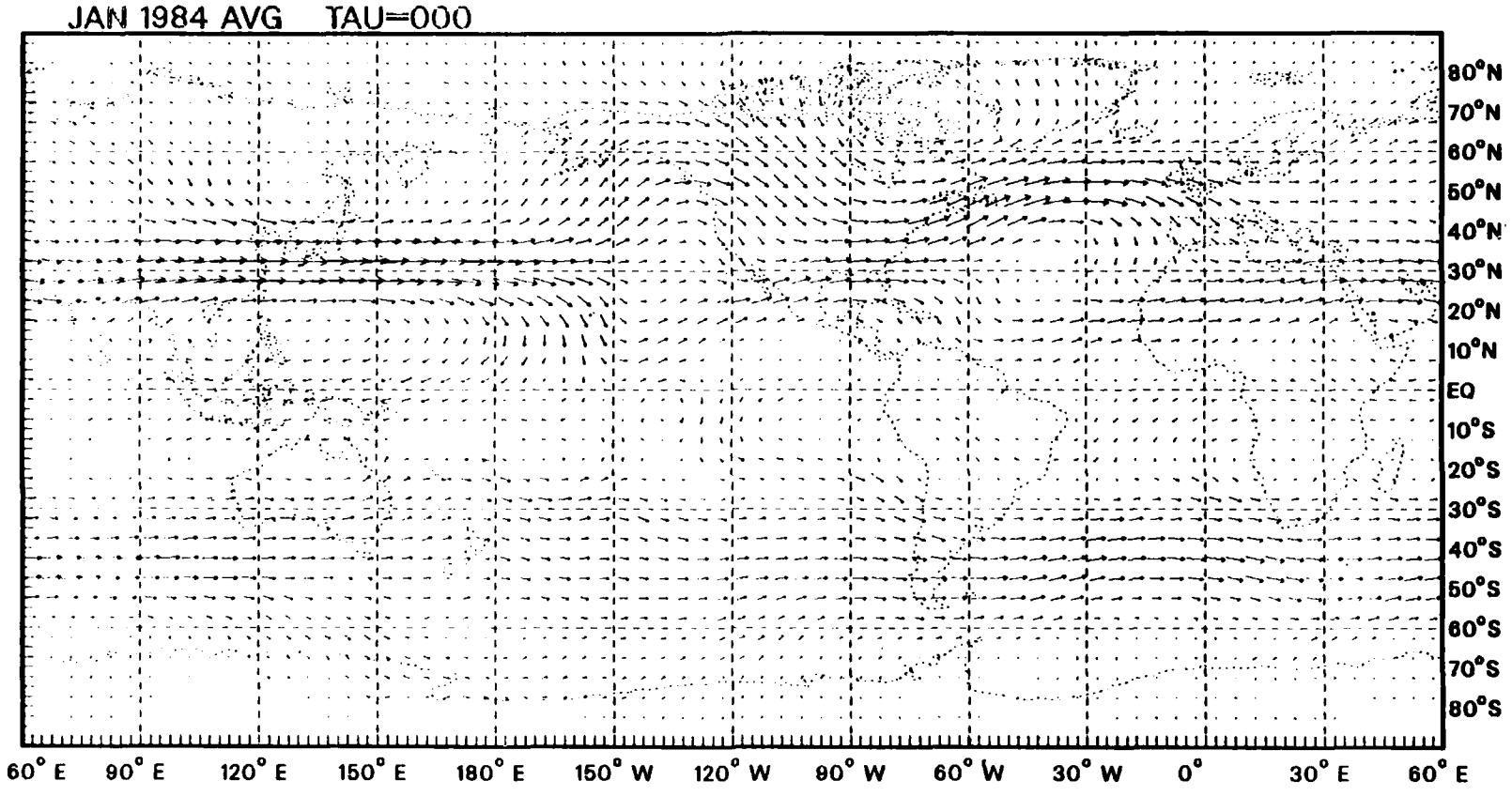

As in Fig. 1A except for the 250 mb wind.

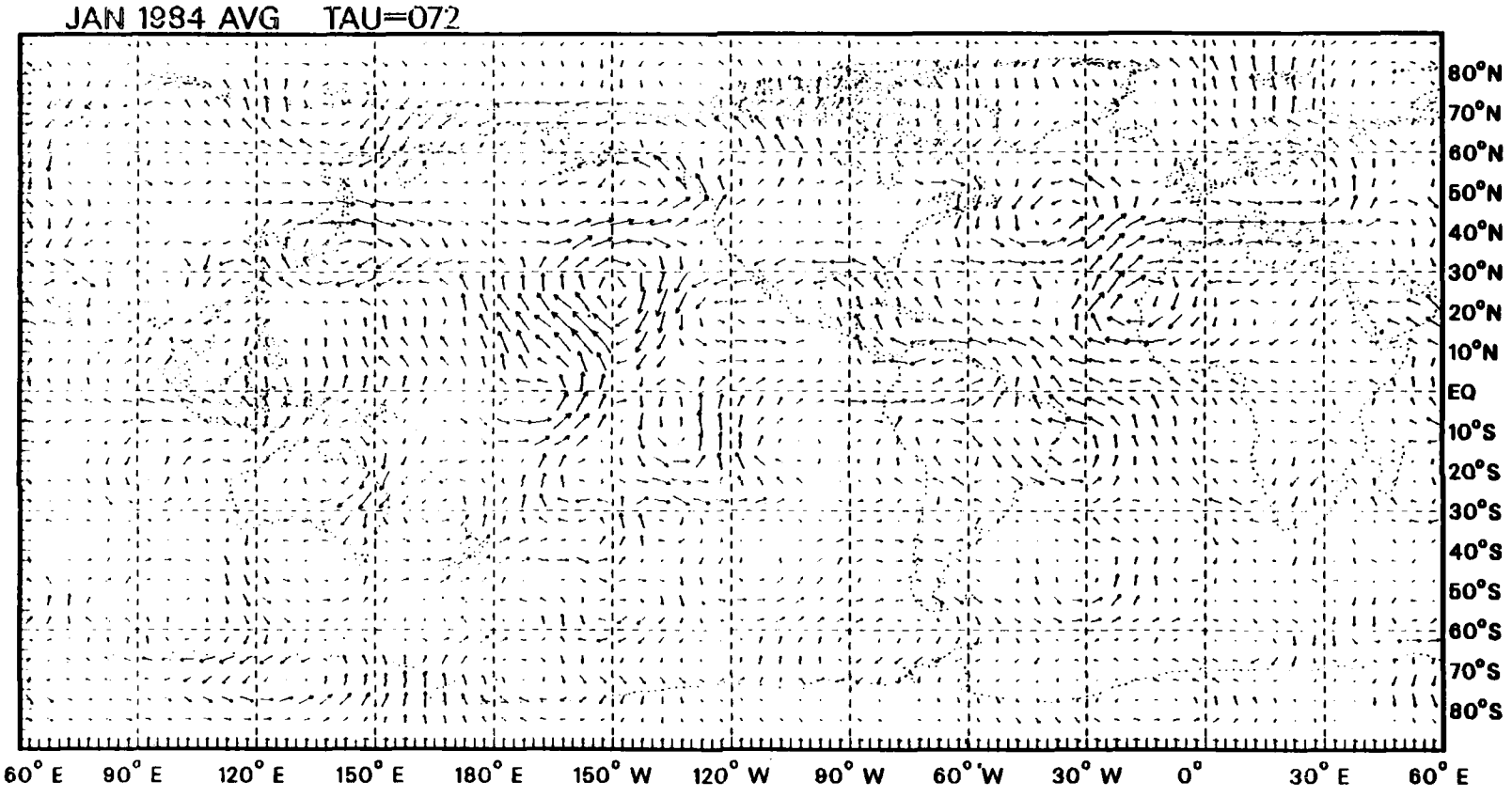

...8 ... m Fig. 18 ... cept for the 250 mb wind.

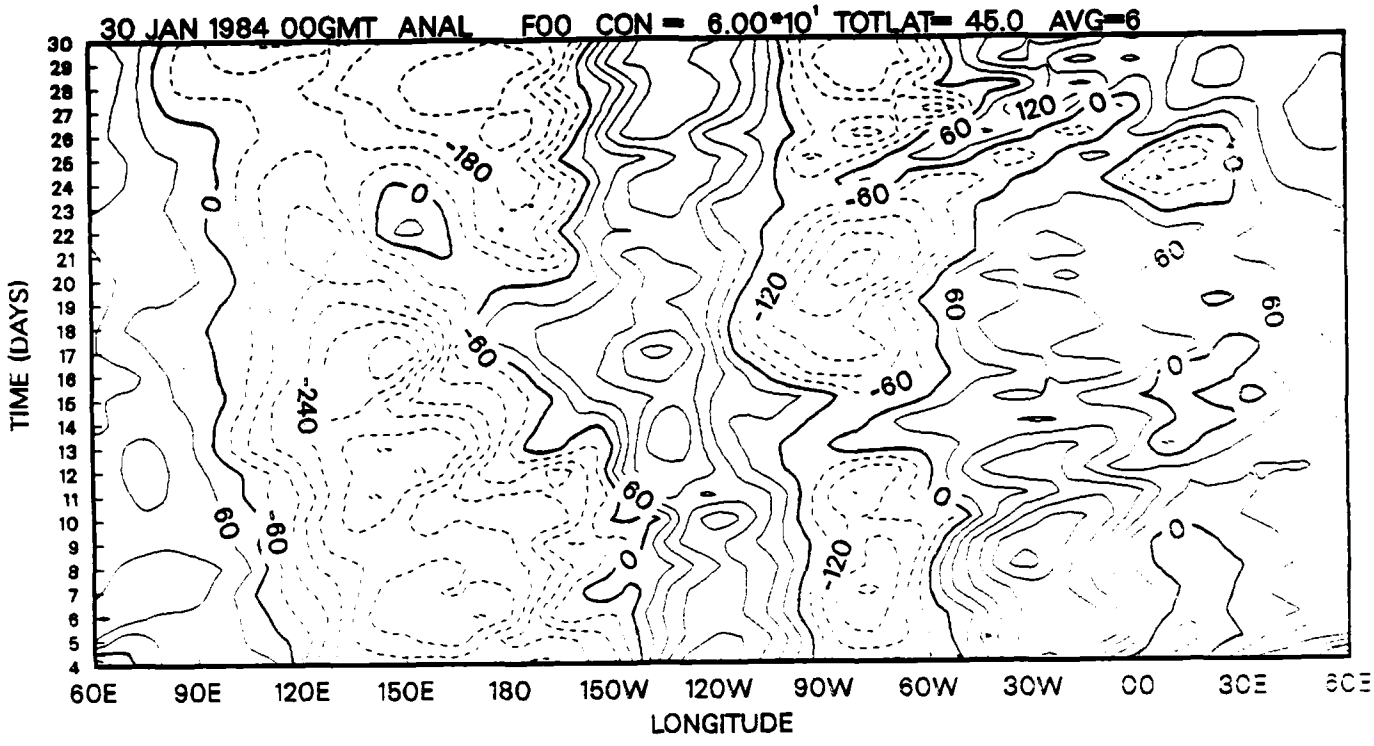

5A Time versus longitude plot (Hovmuller diagram) for the 500 mb geopotential for Jan 1984. The data plotted are average values for the latitude band from 30N to 60N. The contour interval is 50 m.

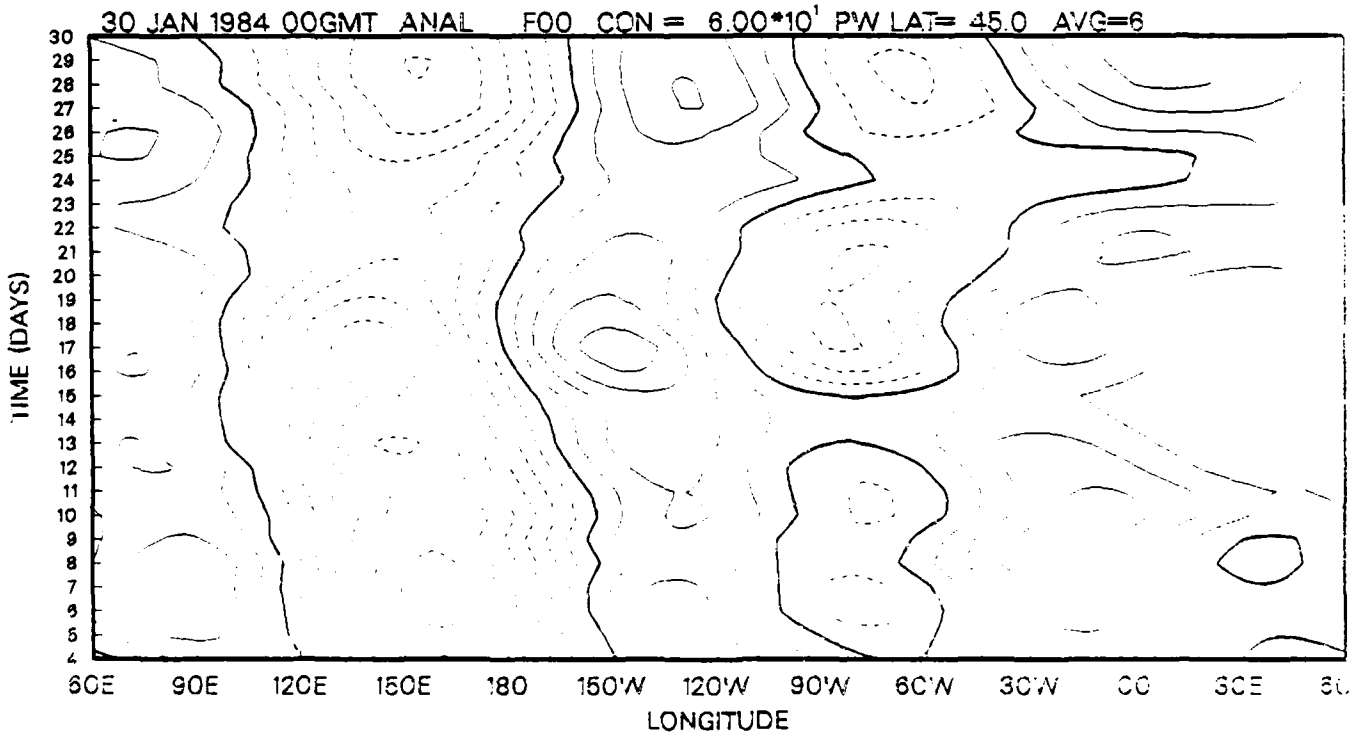

5B As in Fig. 5A except for the planetary scale waves, zonal wave numbers 0 to 3. Contour interval is 50 m.

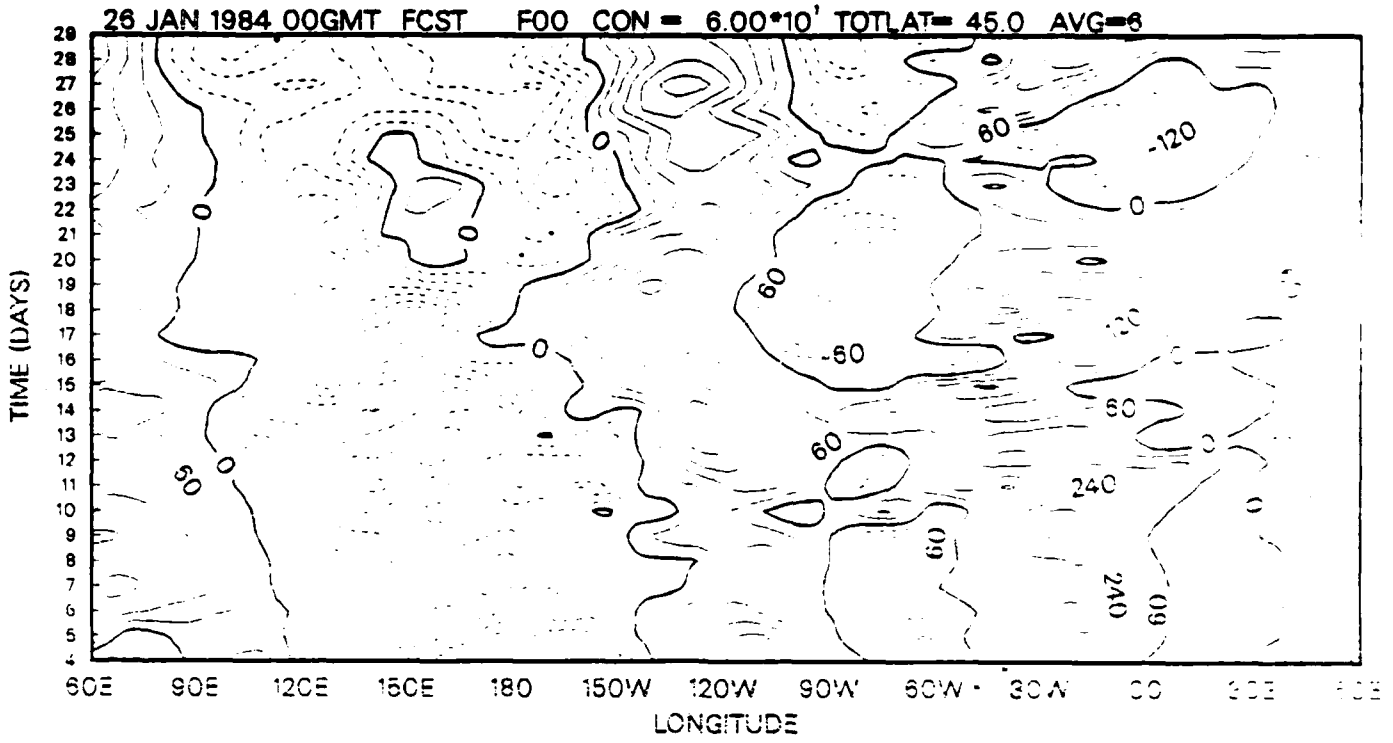

[illegible] as in 6A except for the tau = 36 forecasts. Contour interval is [illegible].

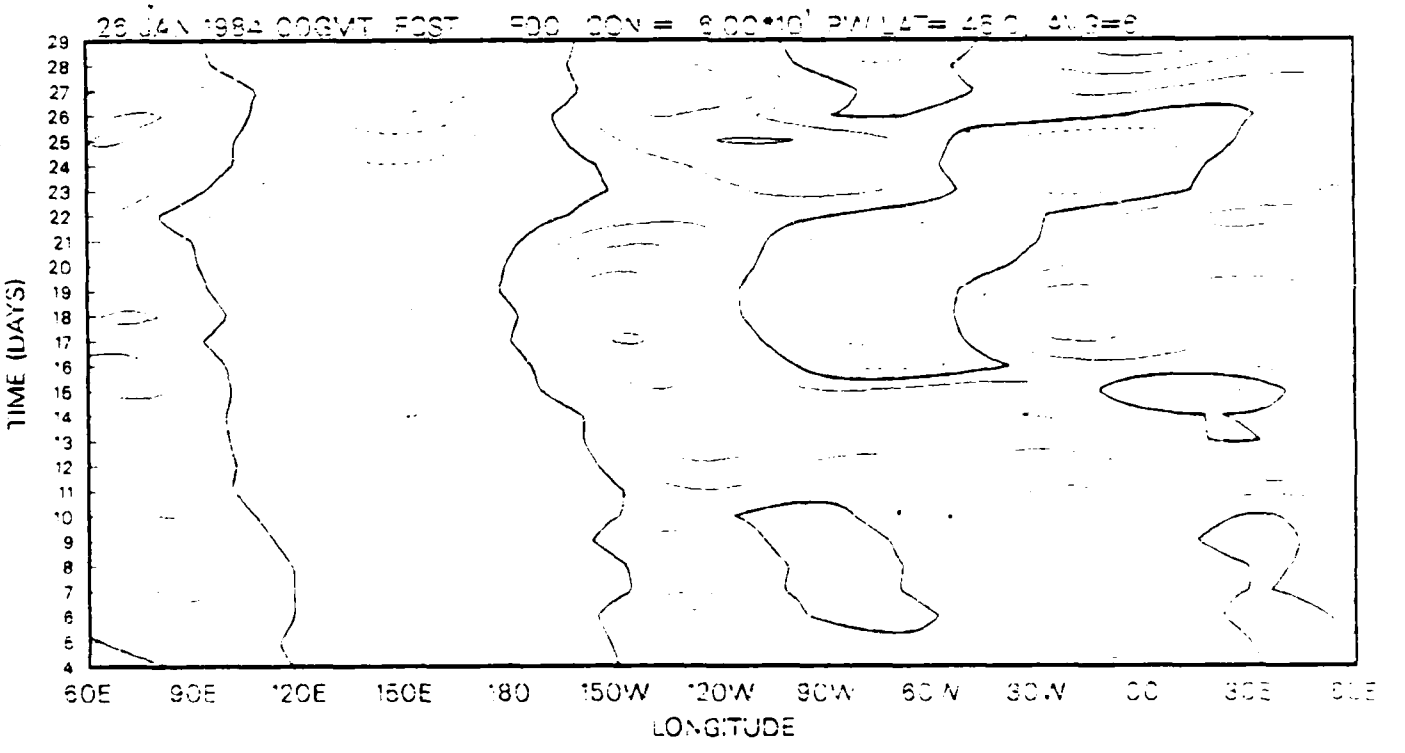

[illegible] as in 6B except for the tau = 36 forecasts. Contour interval is [illegible].

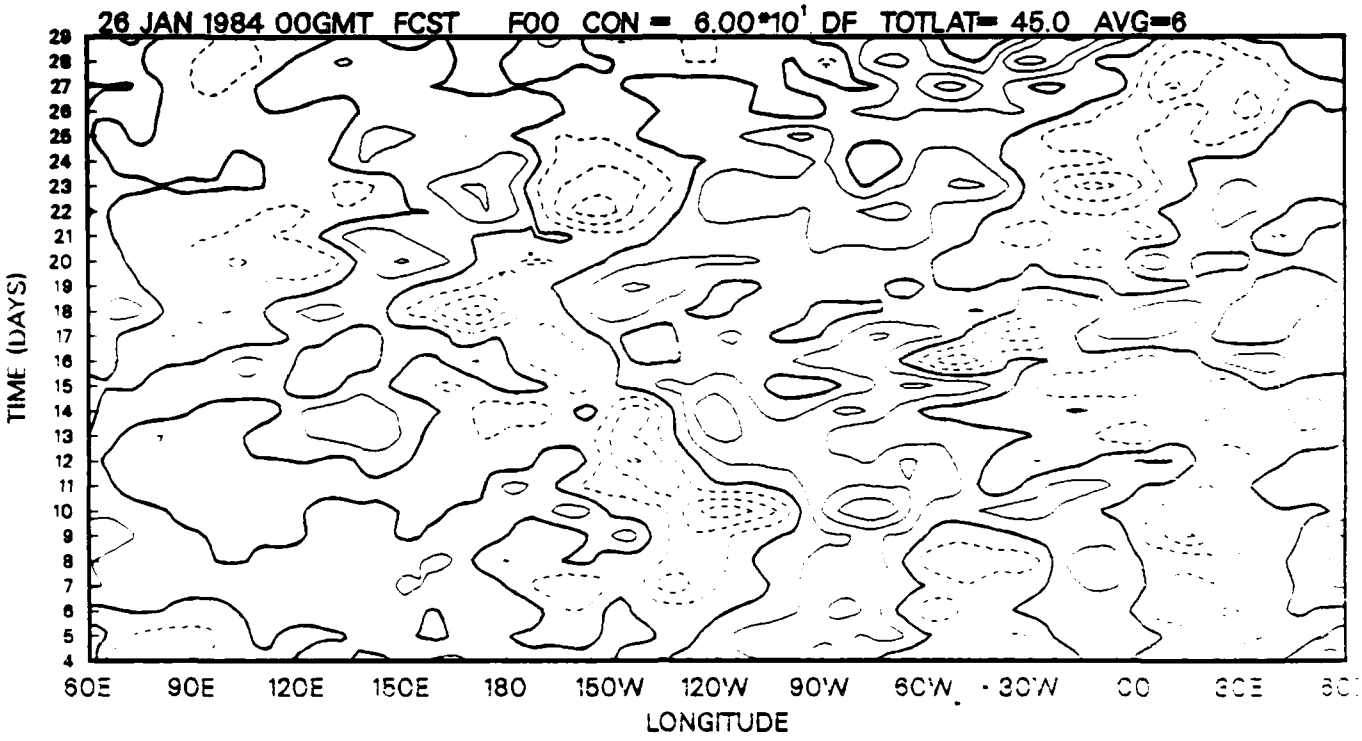

8A As in 6A except for the Tau = 06 forecast error FORECAST [illegible] Contour interval is 60 m.

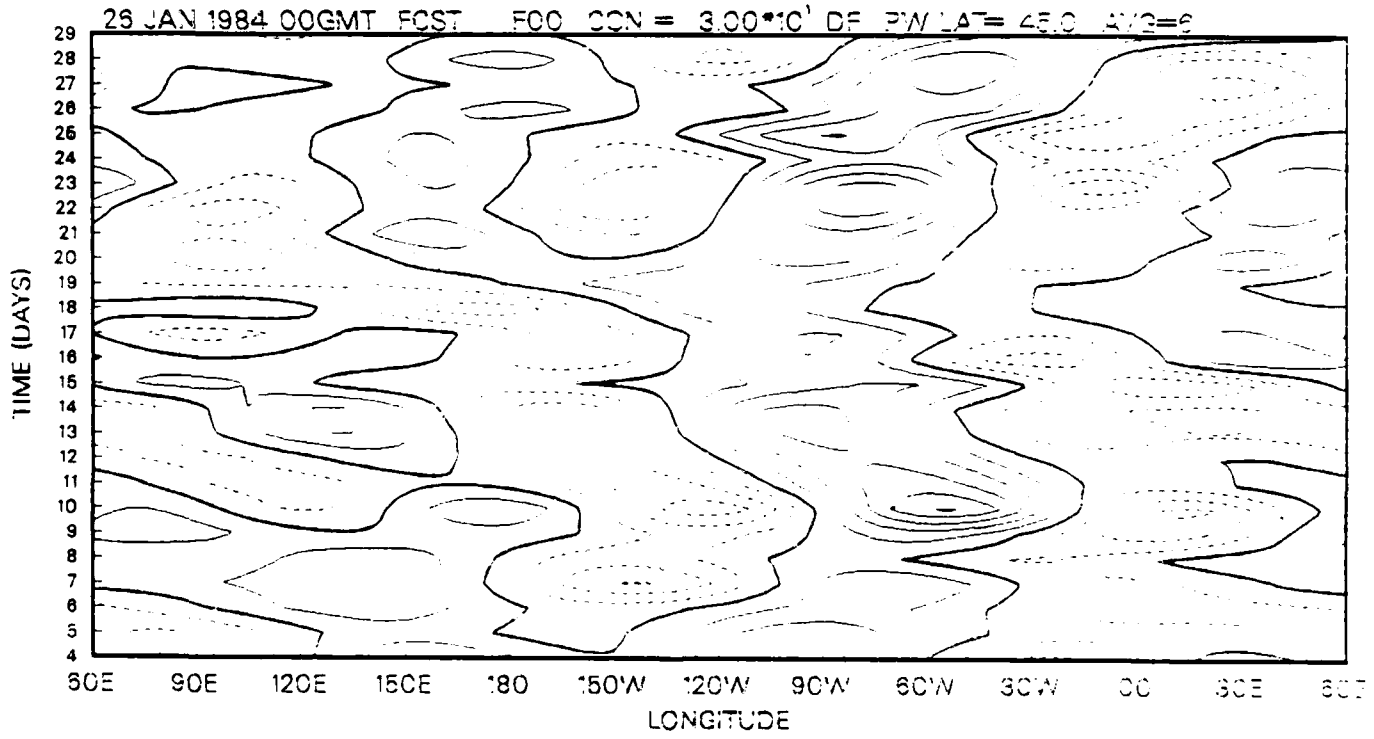

8B As in 8B except for the Tau = 06 h forecast error. Contour [illegible] 30 m.

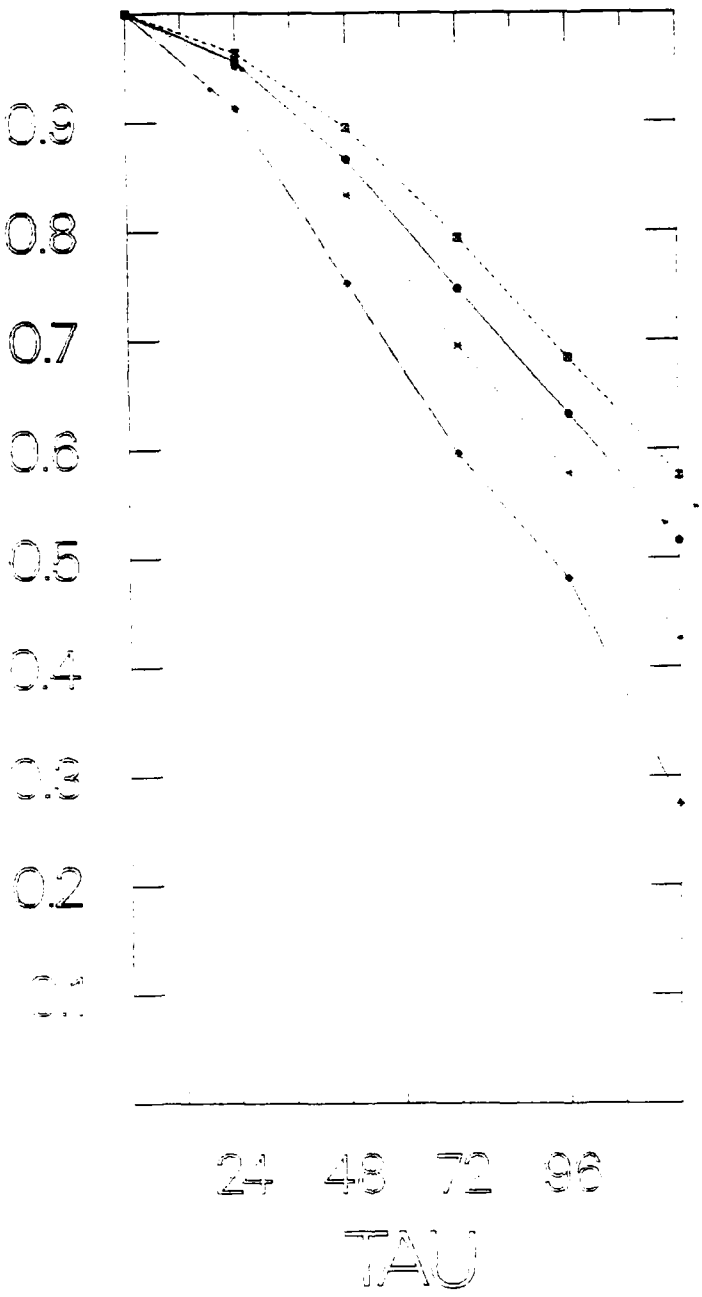

Persistence anomaly correlation for 500 mb geopotential for Northern Hemisphere from 30N to 70N for Jan 1984 for forecast projections out to 96 hours. The ⊠ = planetary waves 1, 2, and 3, ● = total, × = [illegible] waves 4, 5, 6, and 7 and ◆ = synoptic waves 8 to 15.

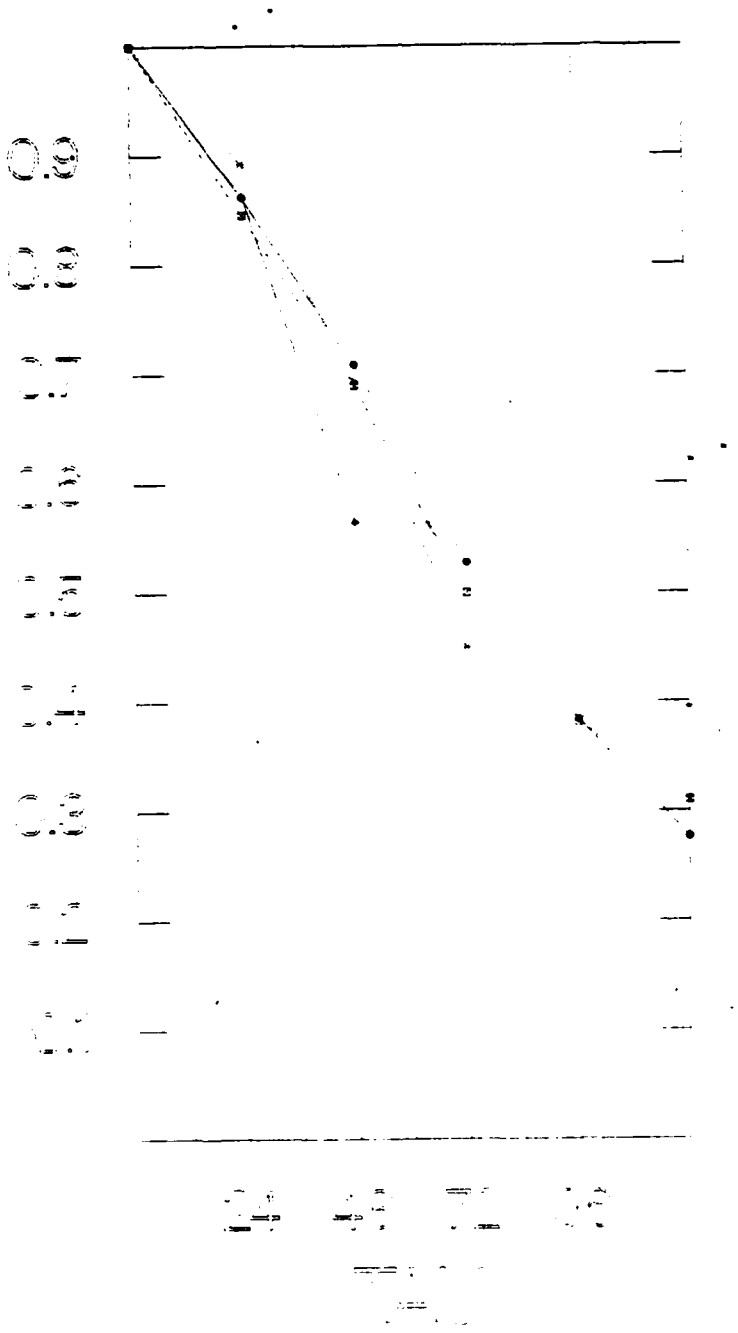

10 ...s in Fig. 9 but for the latitude band 30N to the equator.

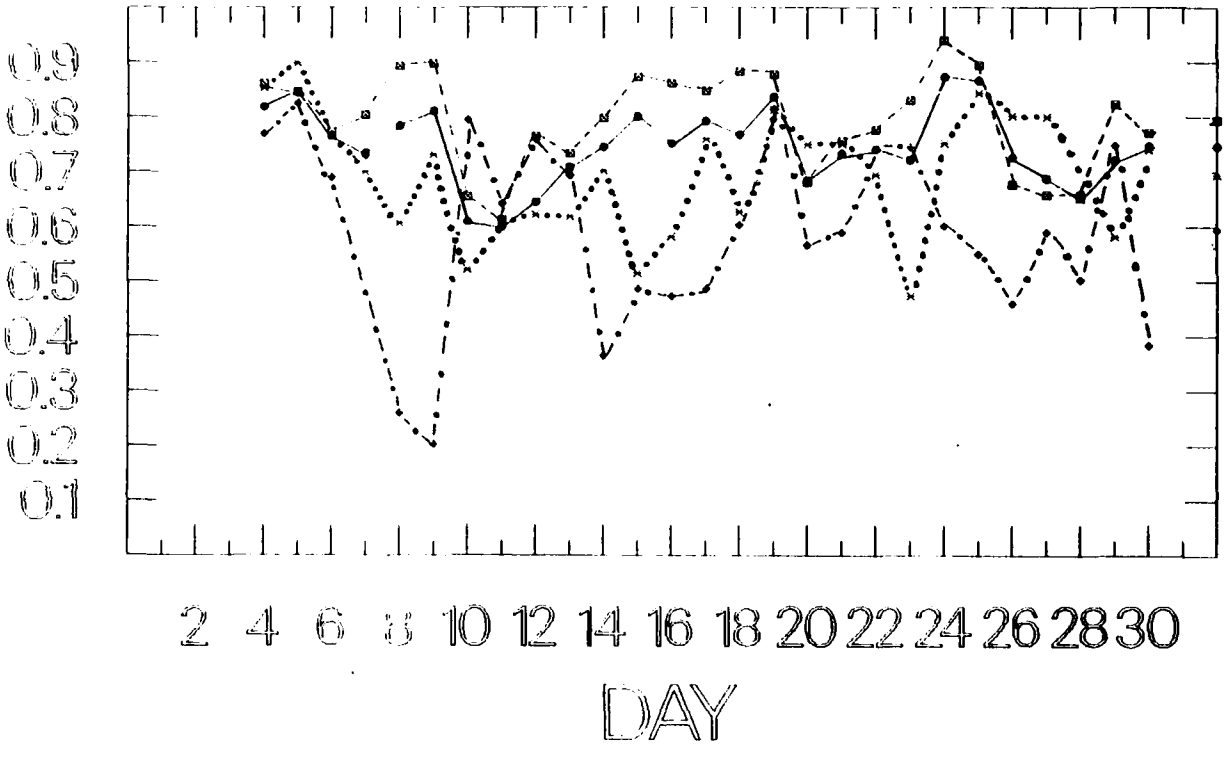

11 Anomaly correlation for 72 h forecasts for the month of Jan 1984 For the 500 mb geopotential average over the latitude band 30N to 60N. The values on the extreme right hand side (day 32) are the monthly means seen in Fig. 9 □ planetary waves, ● total, ◇ long waves and ◇ ultra long waves.

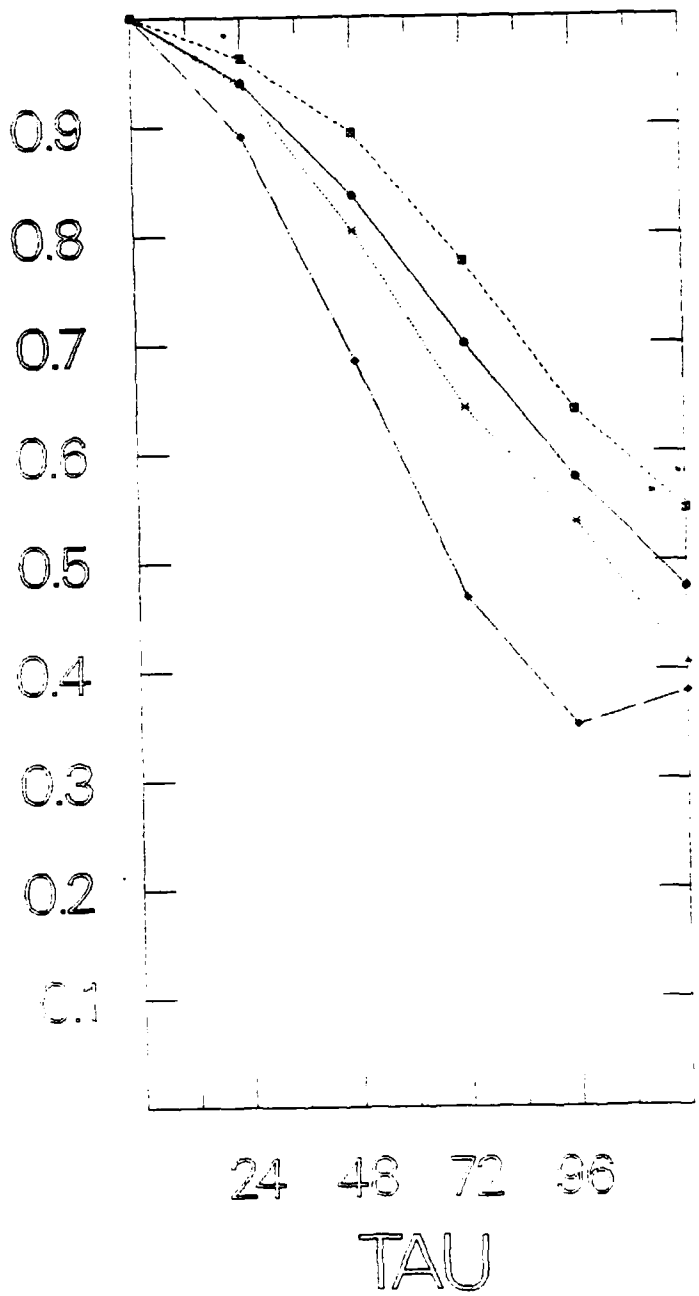

12 As in Fig. 9 but for the 925–500 mb thickness.

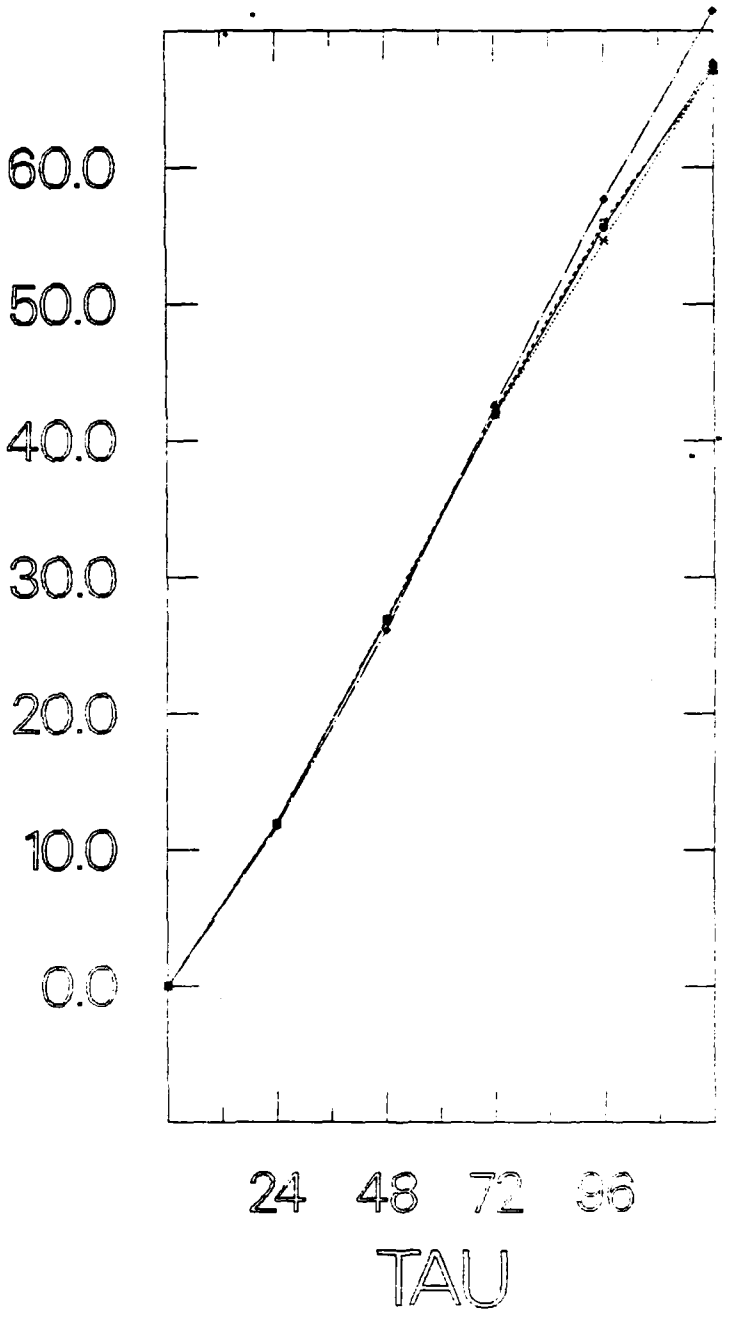

13A Mean error for the 925-500 mb thickness for the latitude band [illegible] for Jan 1984.

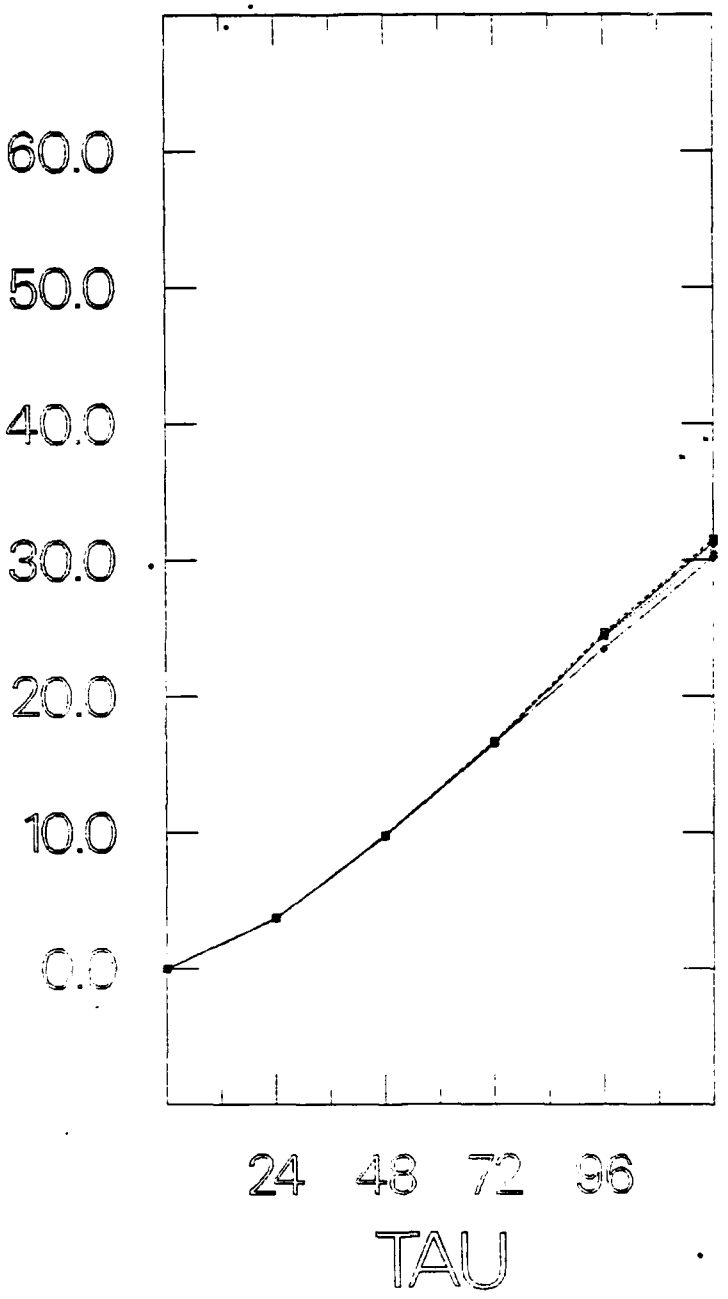

13B As in Fig. 13A except for the latitude band 60N to 70N.

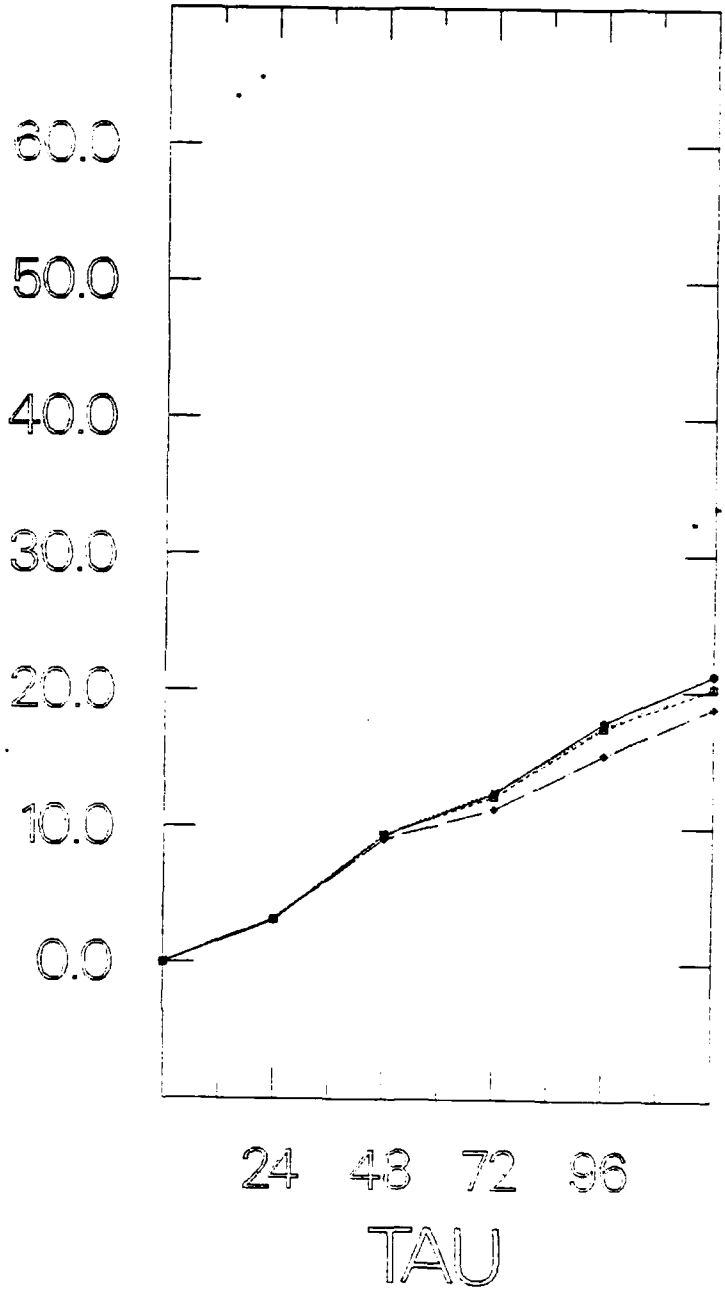

13C As in Fig. 13B except for the latitude band 30N to equator.

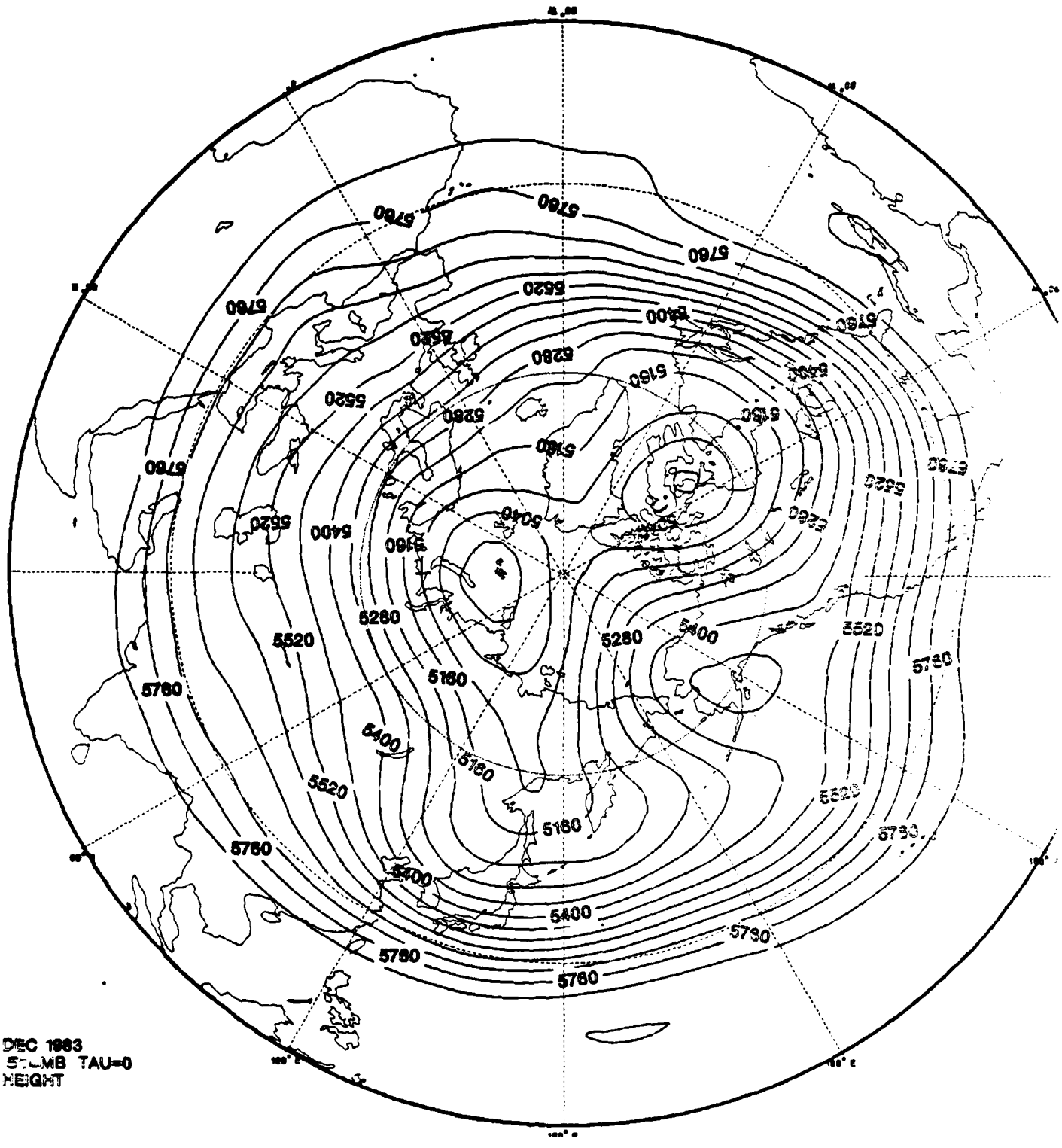

11A As in Fig. 1A except Dec 1983. Contour interval is 60 m.

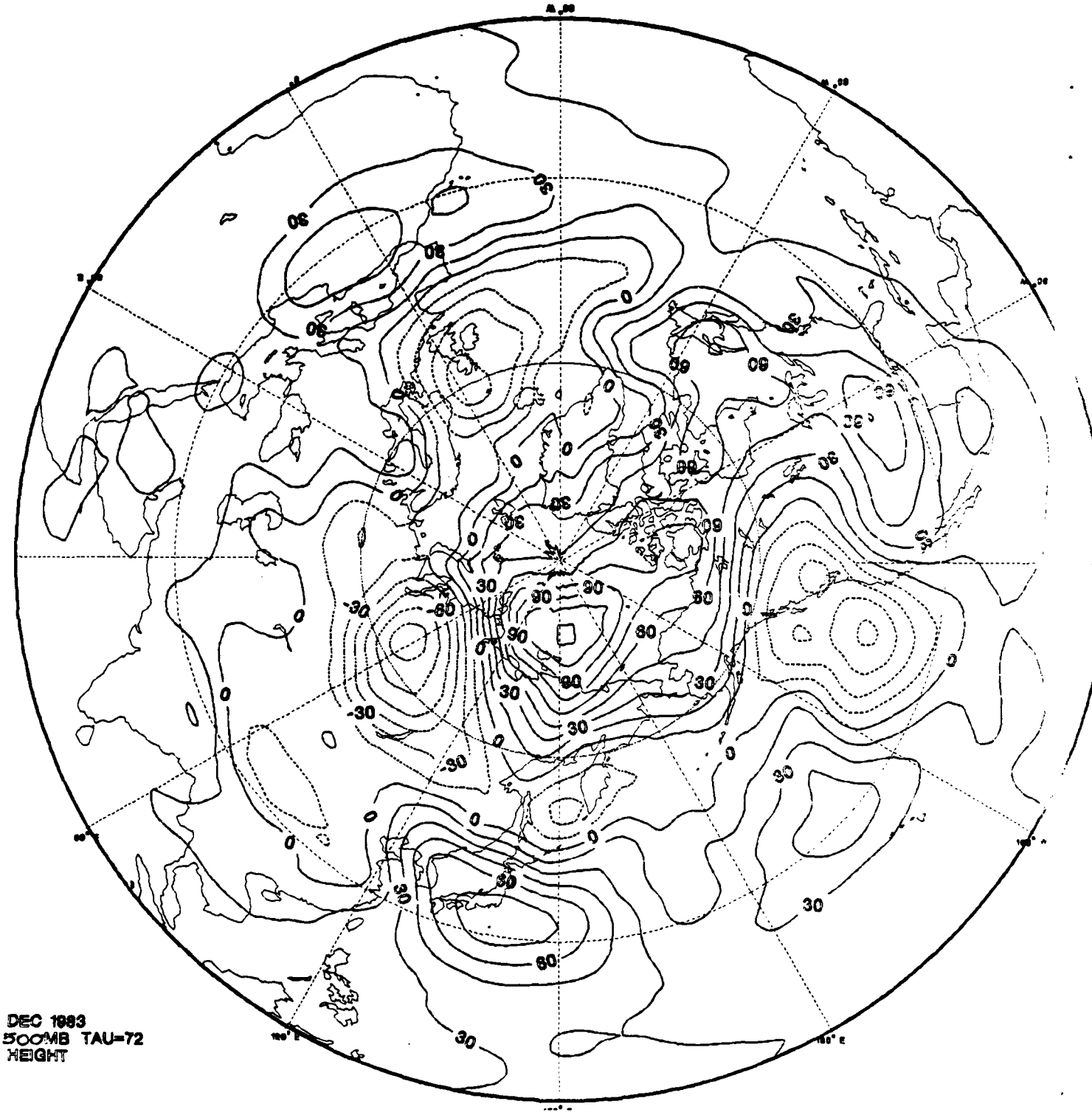

14B As in Fig. 1C except Dec 1983. Contour interval is 15 m.

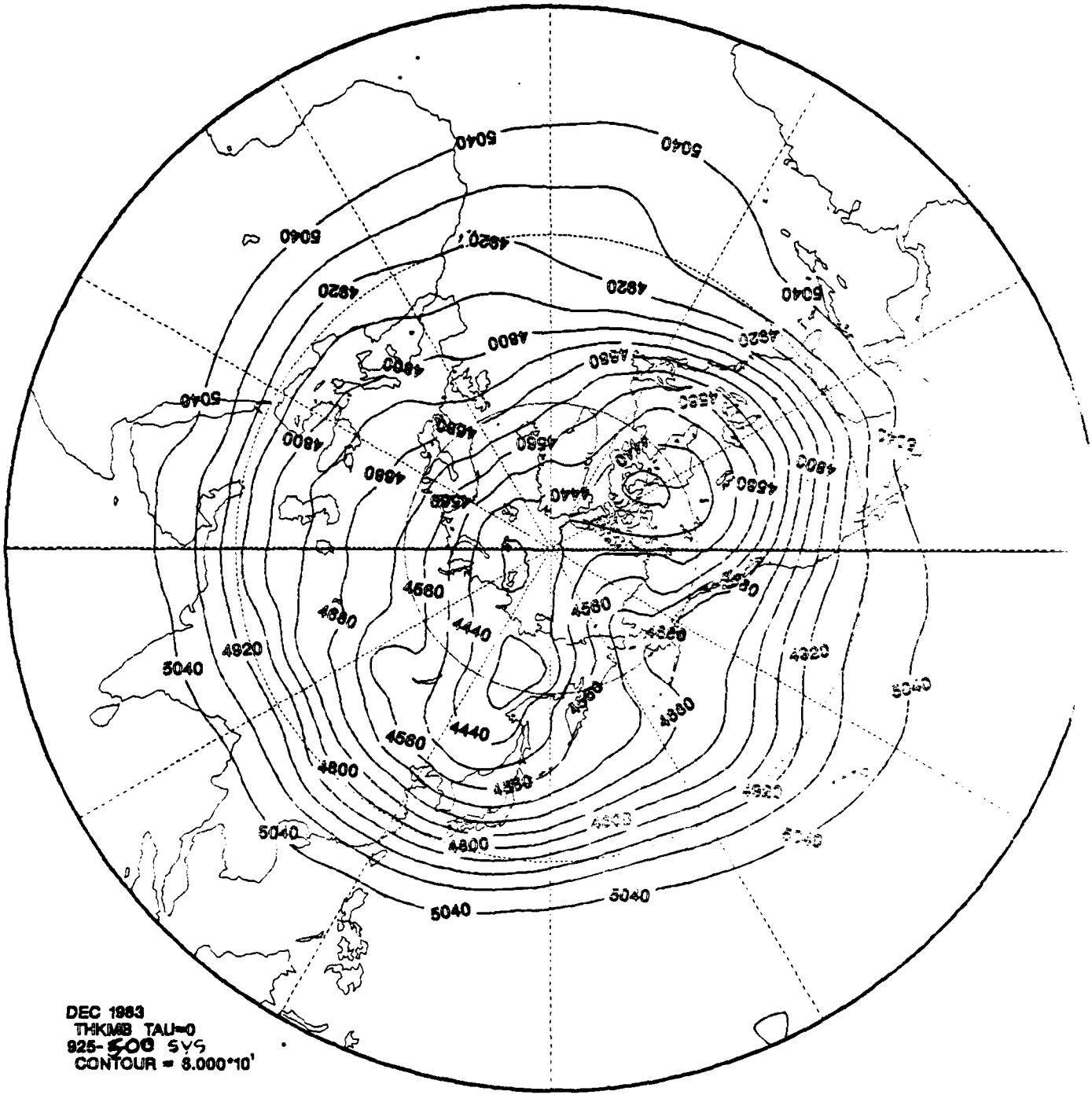

15A As in Fig. 2A except Dec 1983. Contour interval is 60 m.

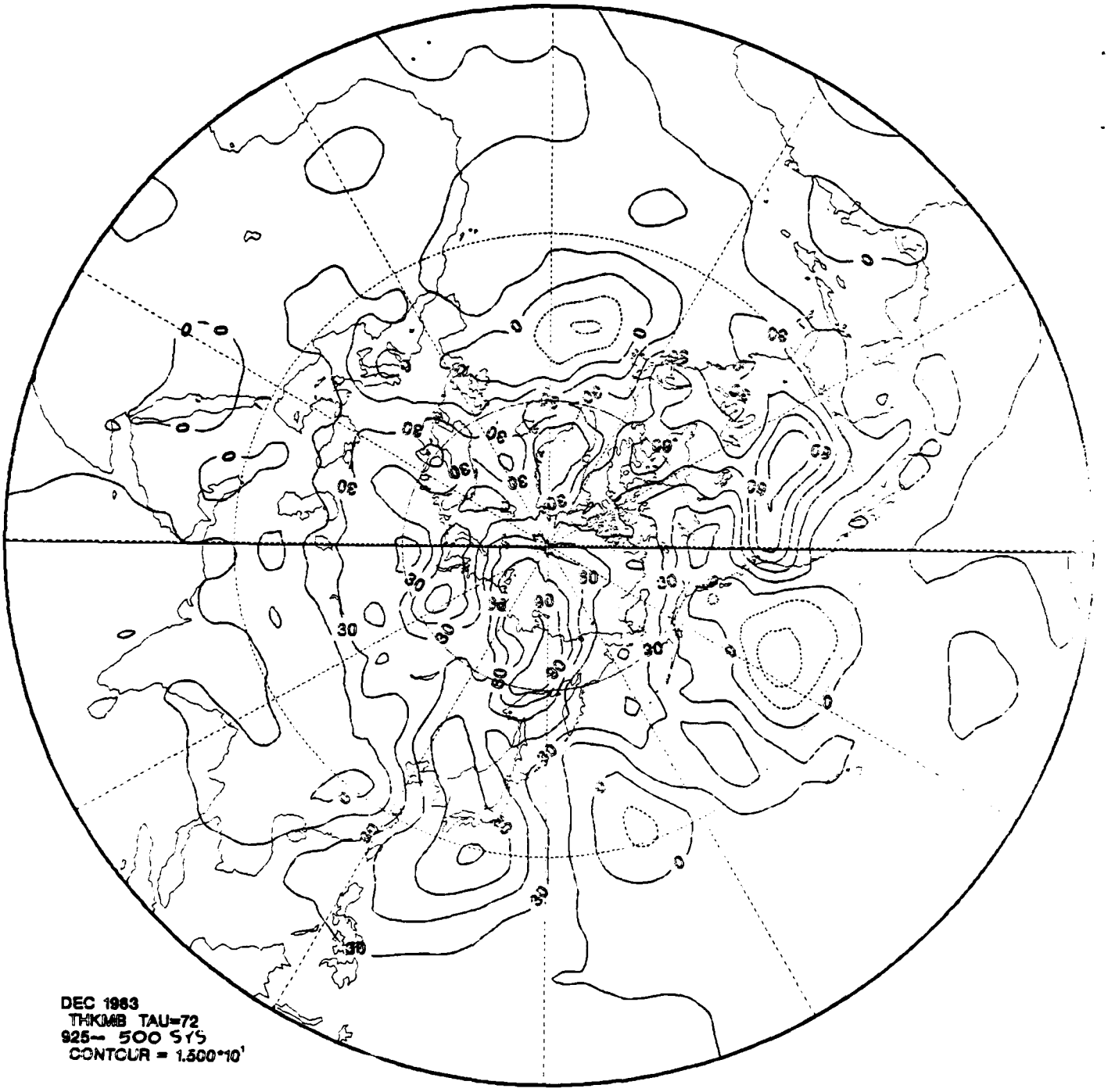

15B As in Fig. 2B except Dec 1983. Contour interval is 15 m.

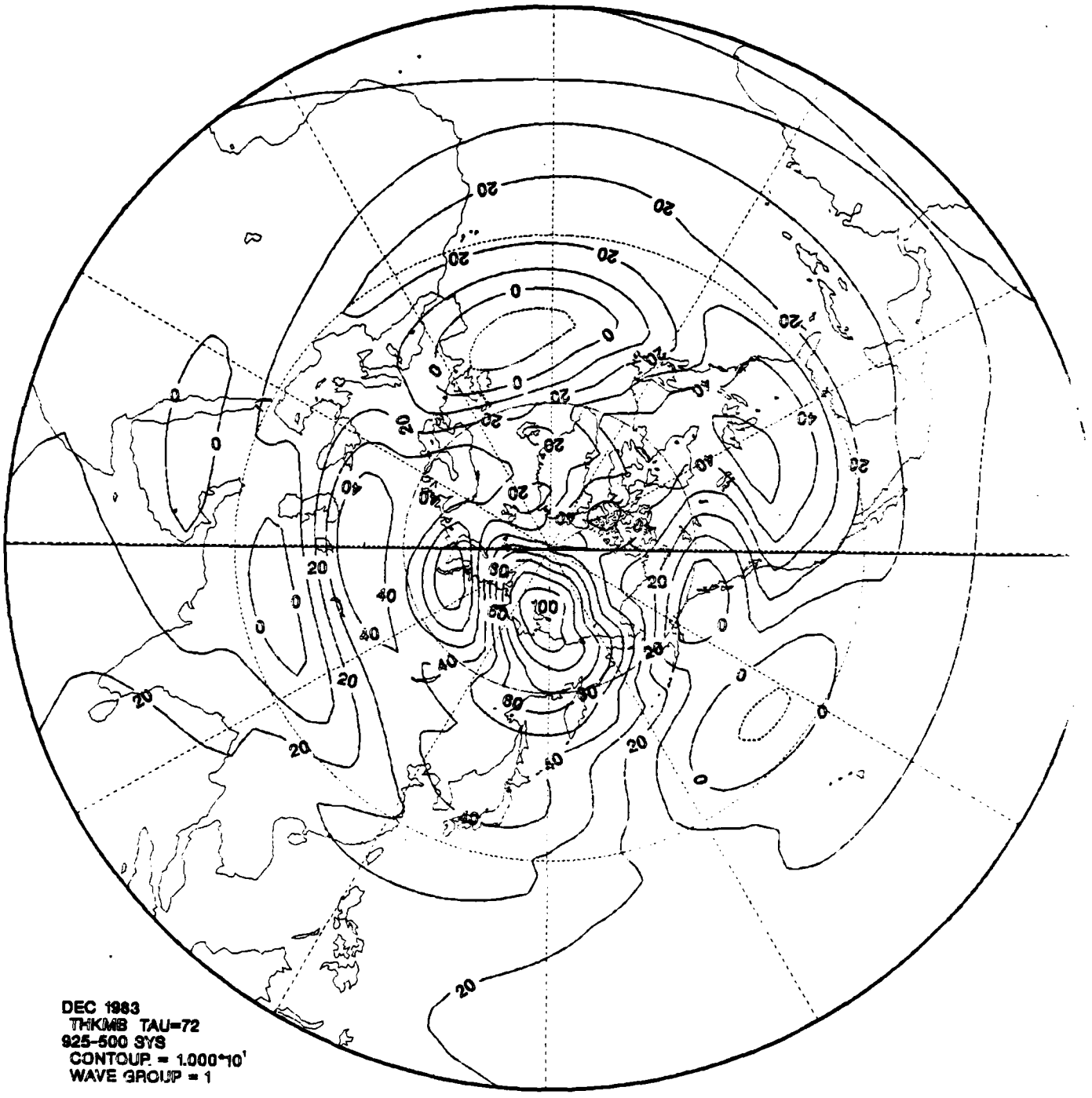

15C As in Fig. 2C except Dec 1983. Contour interval is 10 m.

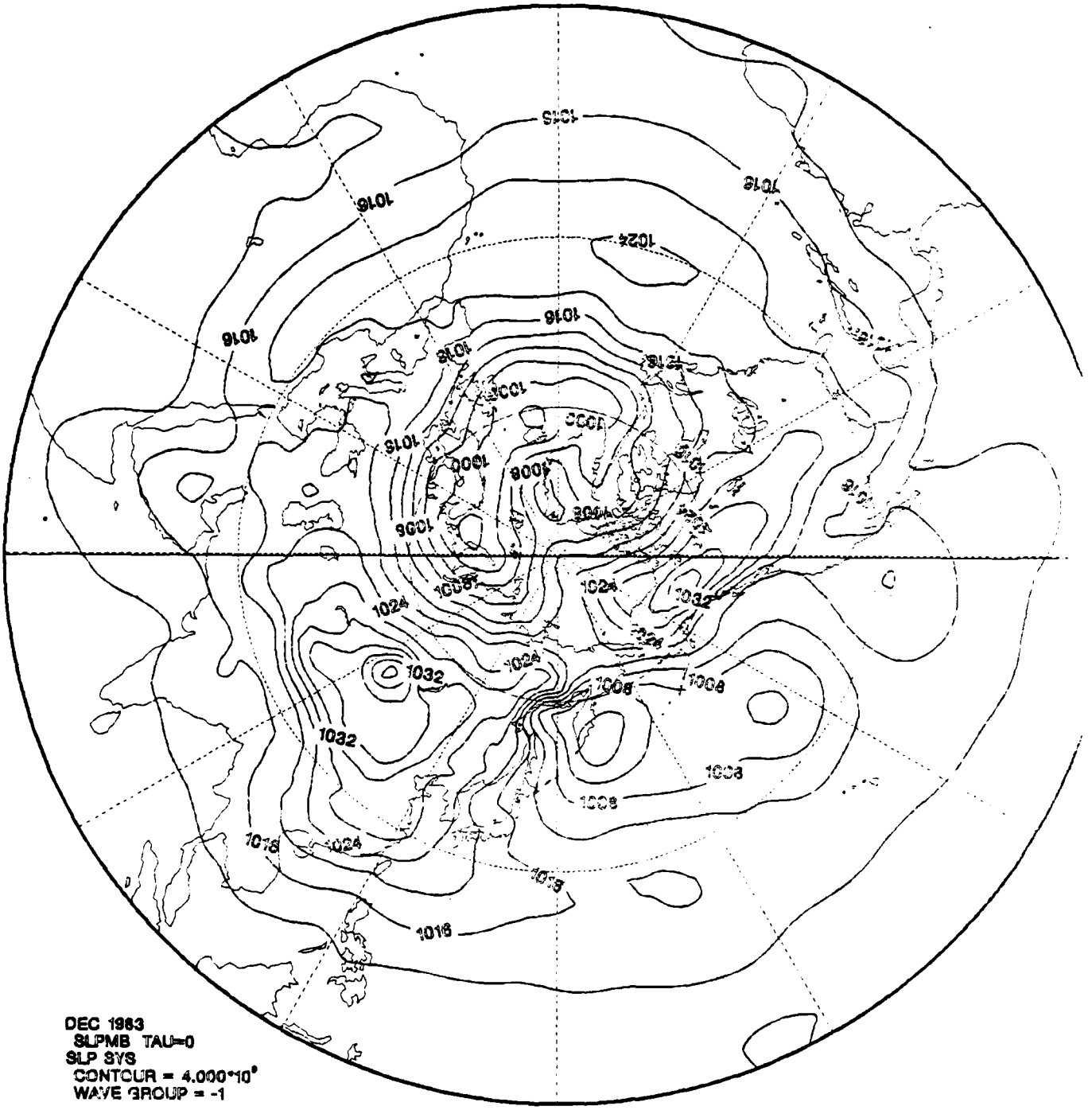

16A As in Fig. 5A except Dec 1983. Contour interval is 4 mb.

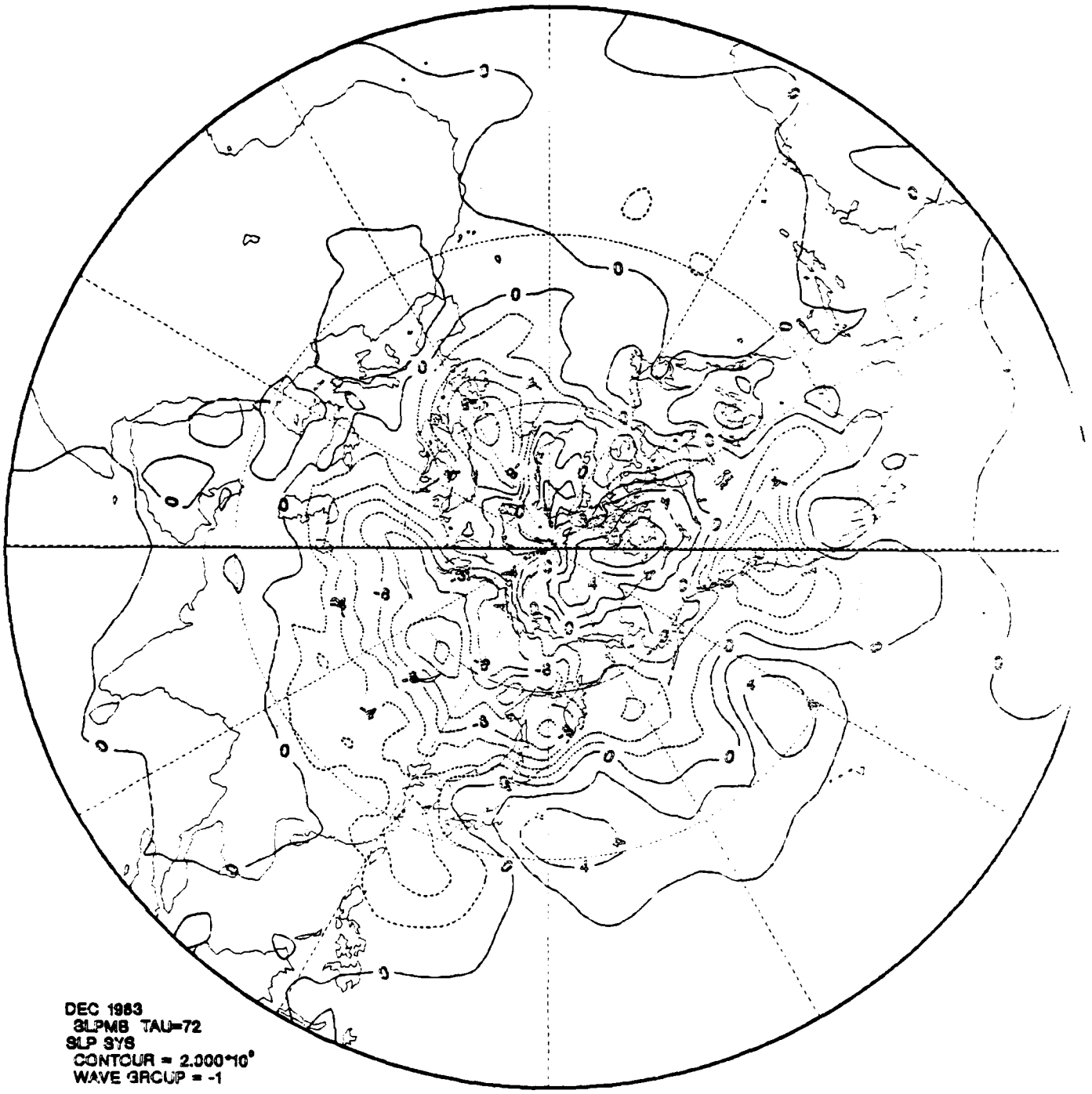

16B As in Fig. 3B except Dec 1983. Contour interval is 2 mb

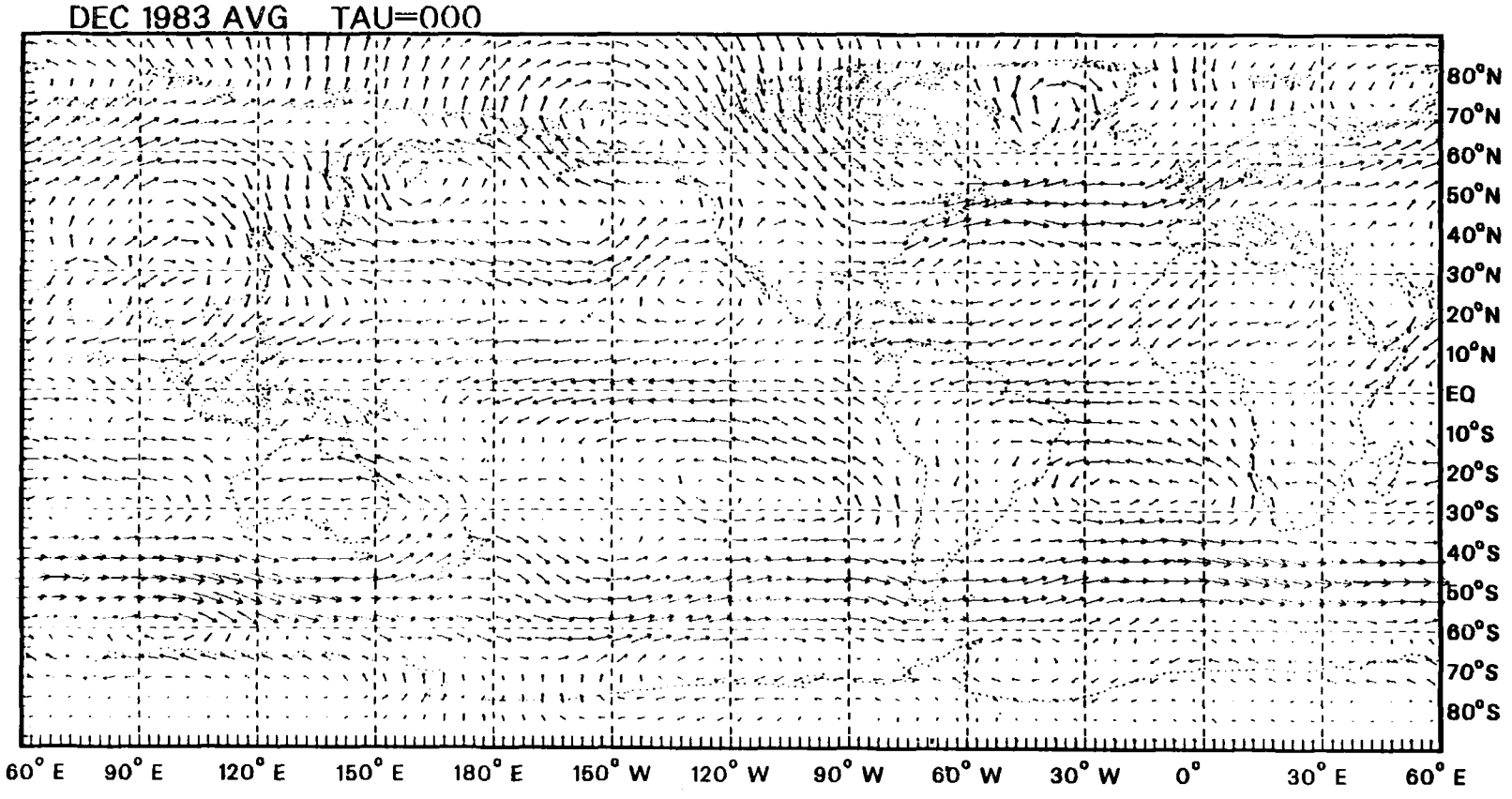

Fig. IX-4b Same as Fig. IX-4a except Dec 1983.

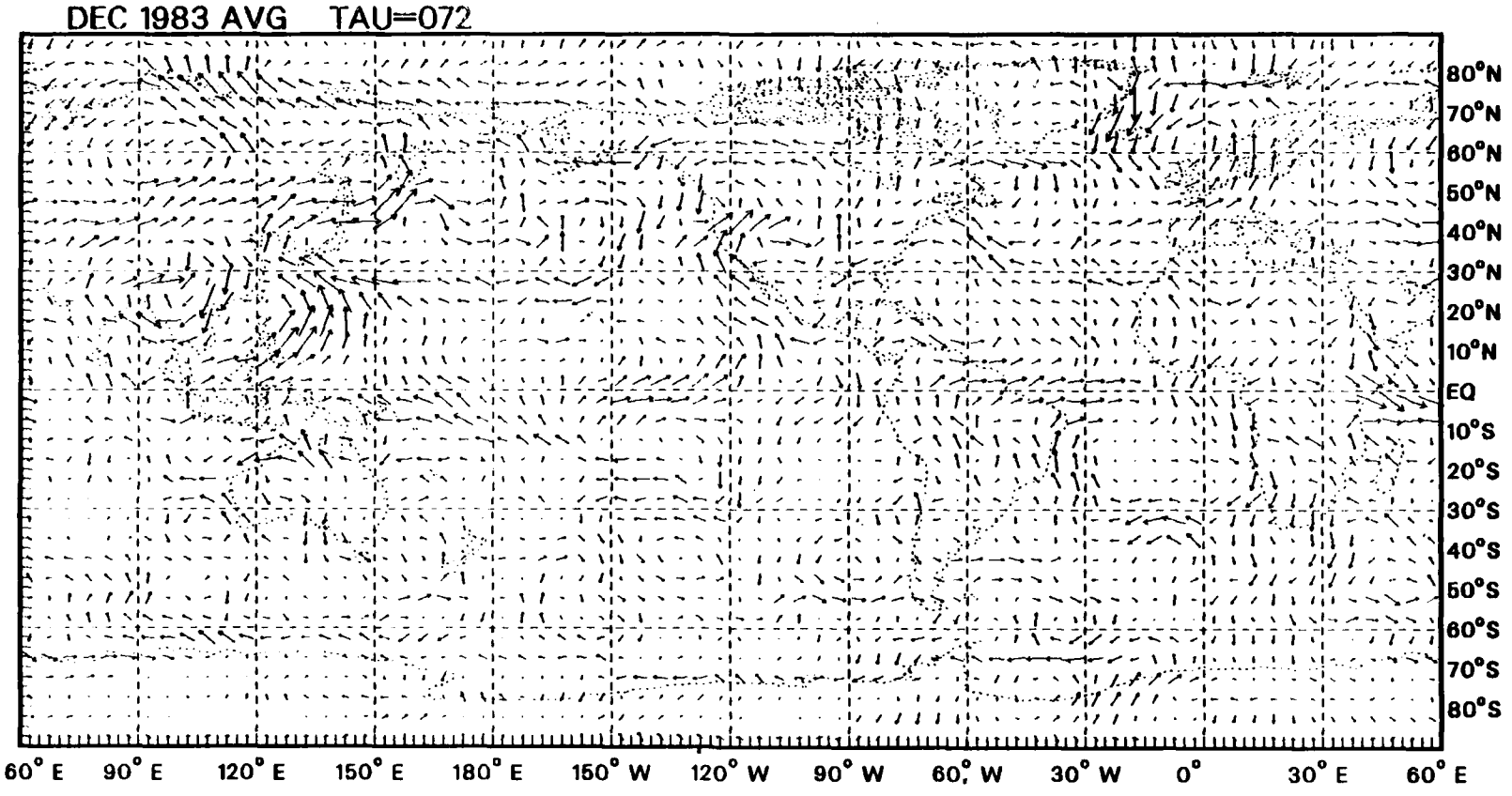

Fig. As in Fig. 18, except Dec 1983.

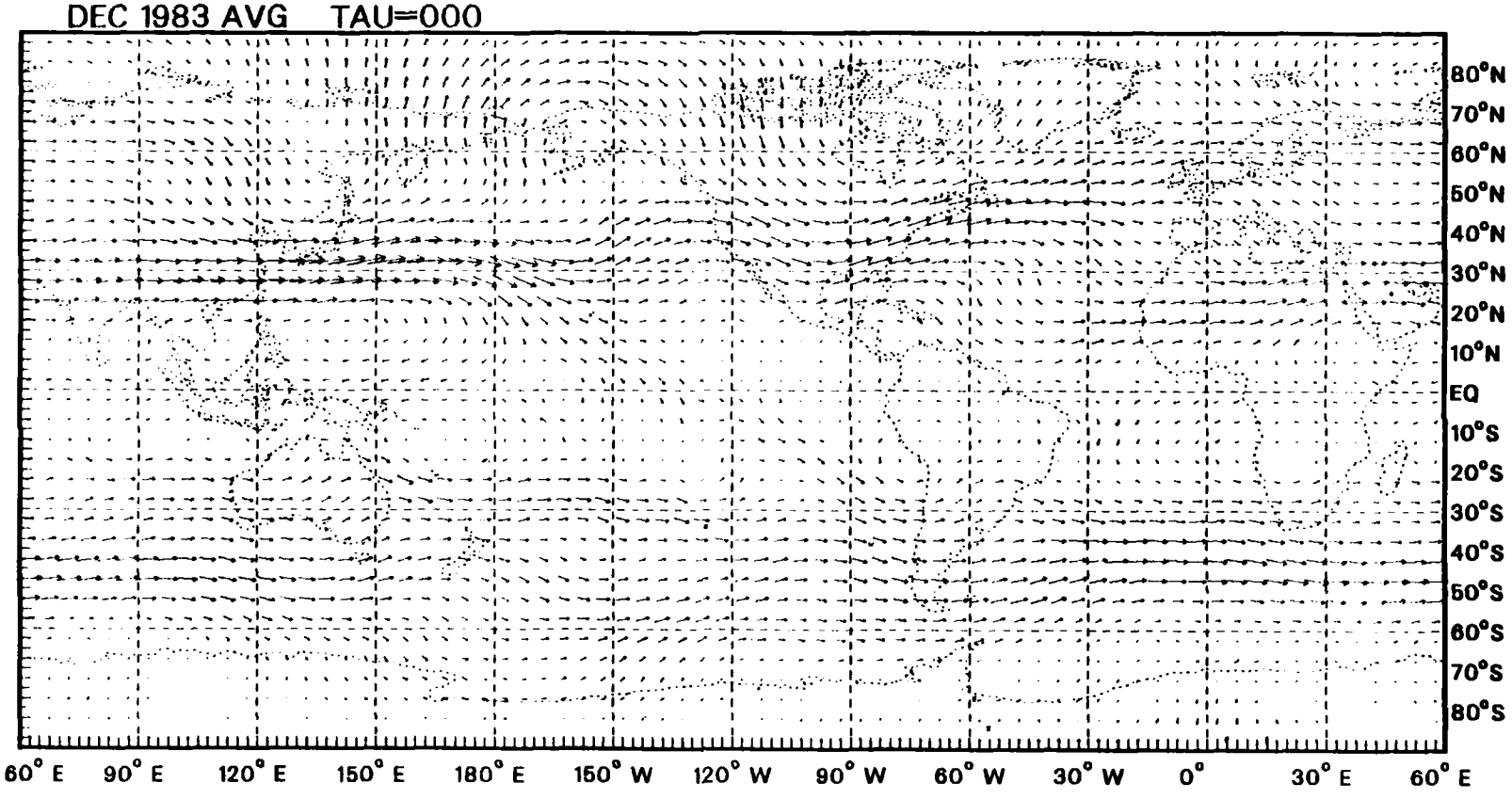
DEC 1983 AVG TAU=000
80°N
70°N
60°N
50°N
40°N
30°N
20°N
10°N
EQ
10°S
20°S
30°S
40°S
50°S
60°S
70°S
80°S
60° E
90° E
120° E
150° E
180° E
150° W
120° W
90° W
60° W
30° W
0°
30° E
60° E

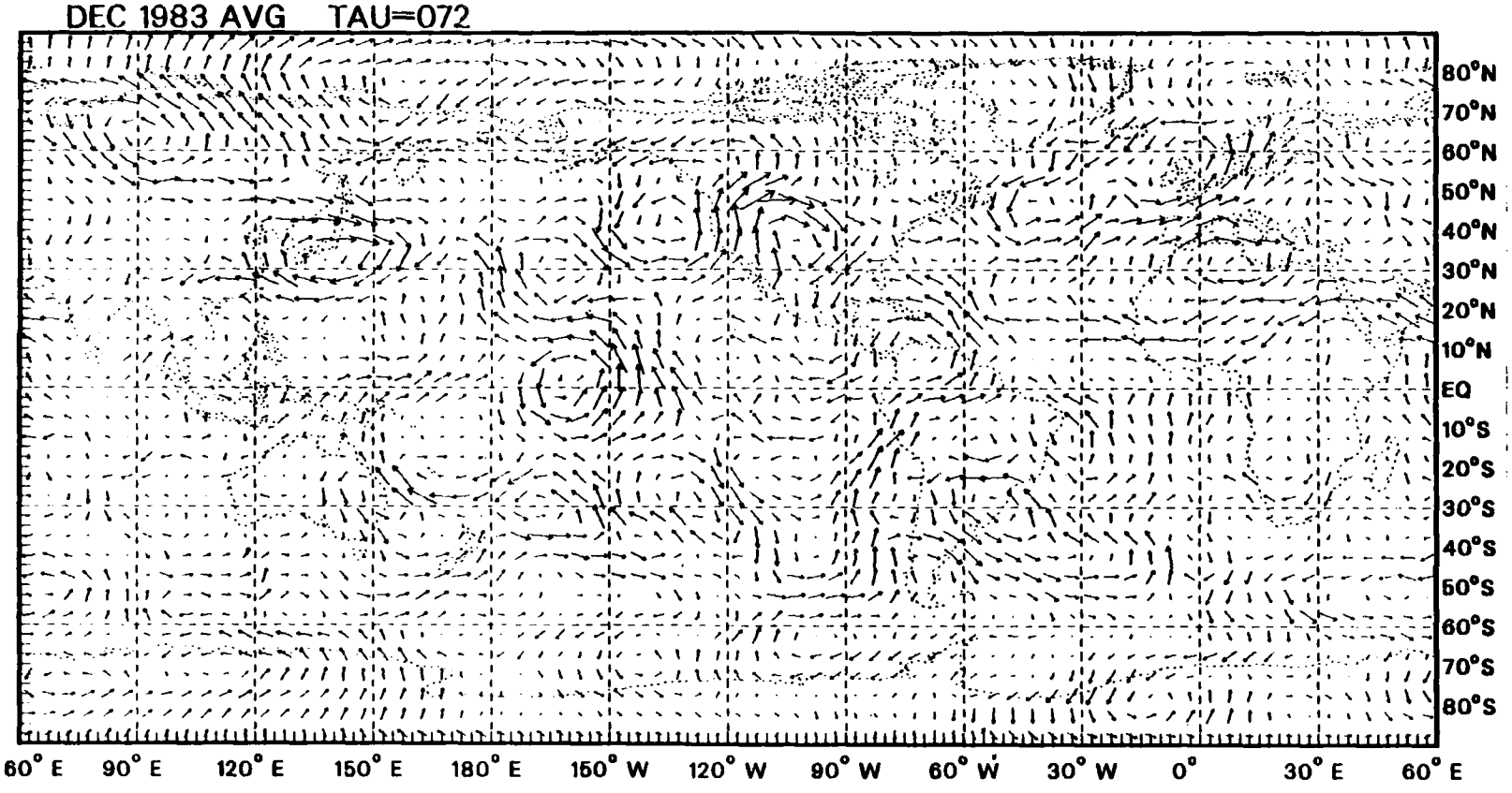

(b) As in Fig. 4B except Dec 1983.

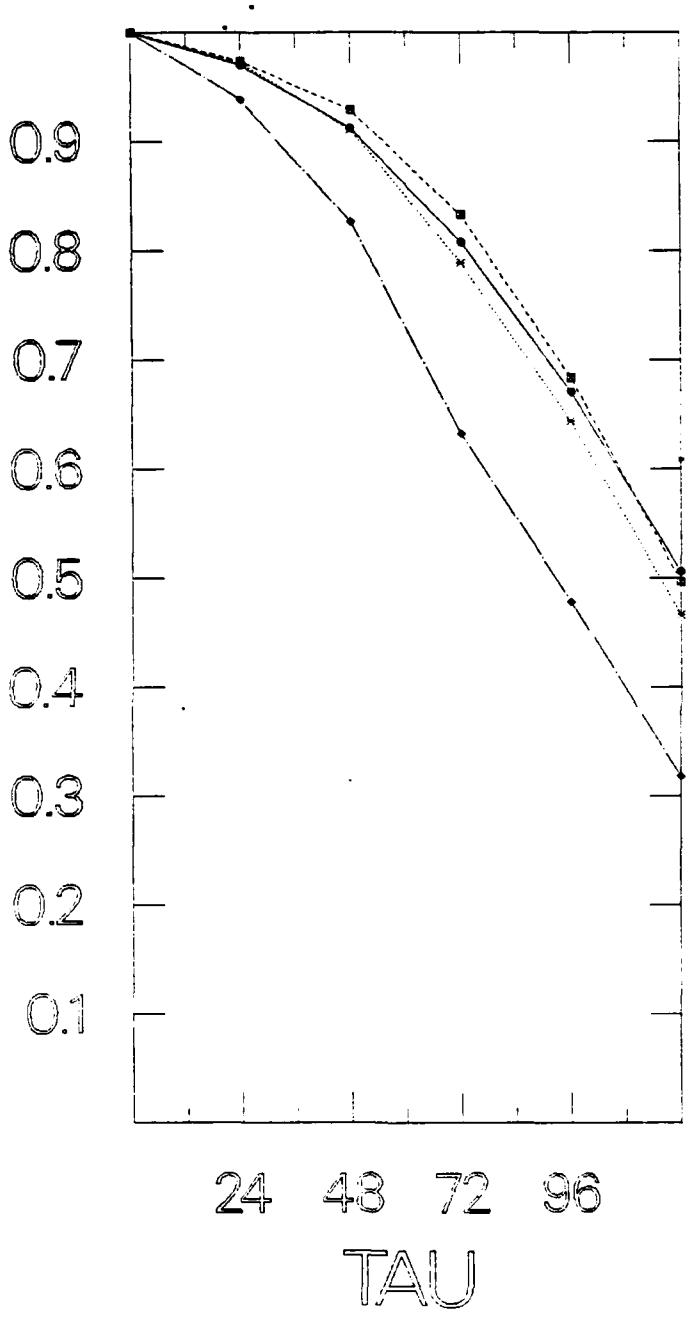

19 As in Fig. 9 but for Dec 1983.

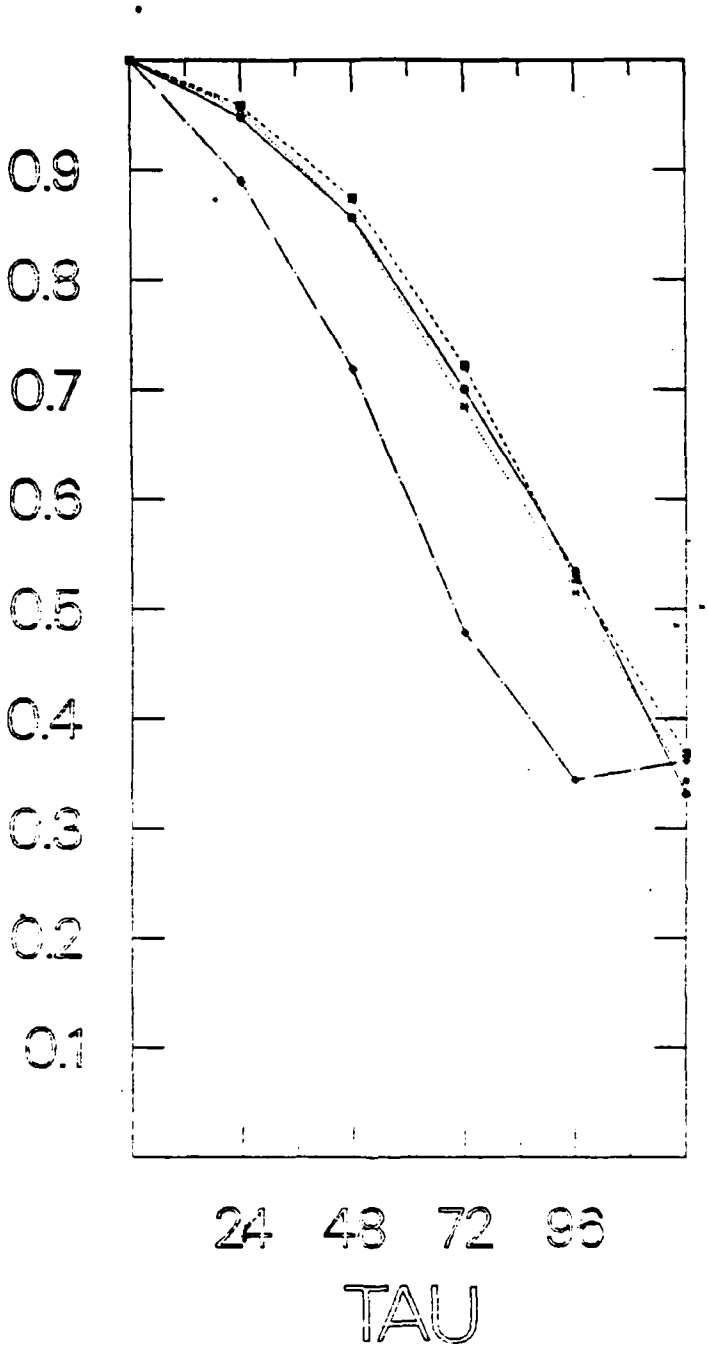

20 As in Fig. 12 but for Dec 1983.

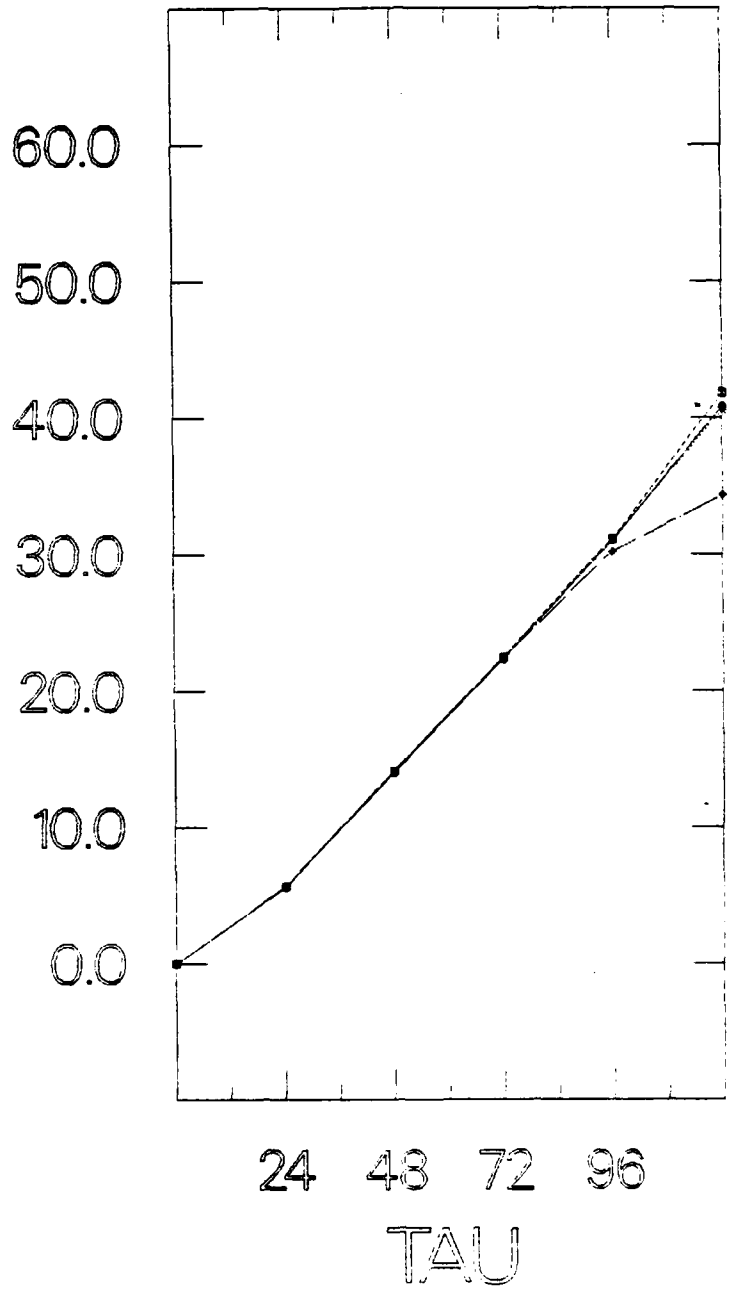

21 As in Fig. 13A but for Dec 1983.

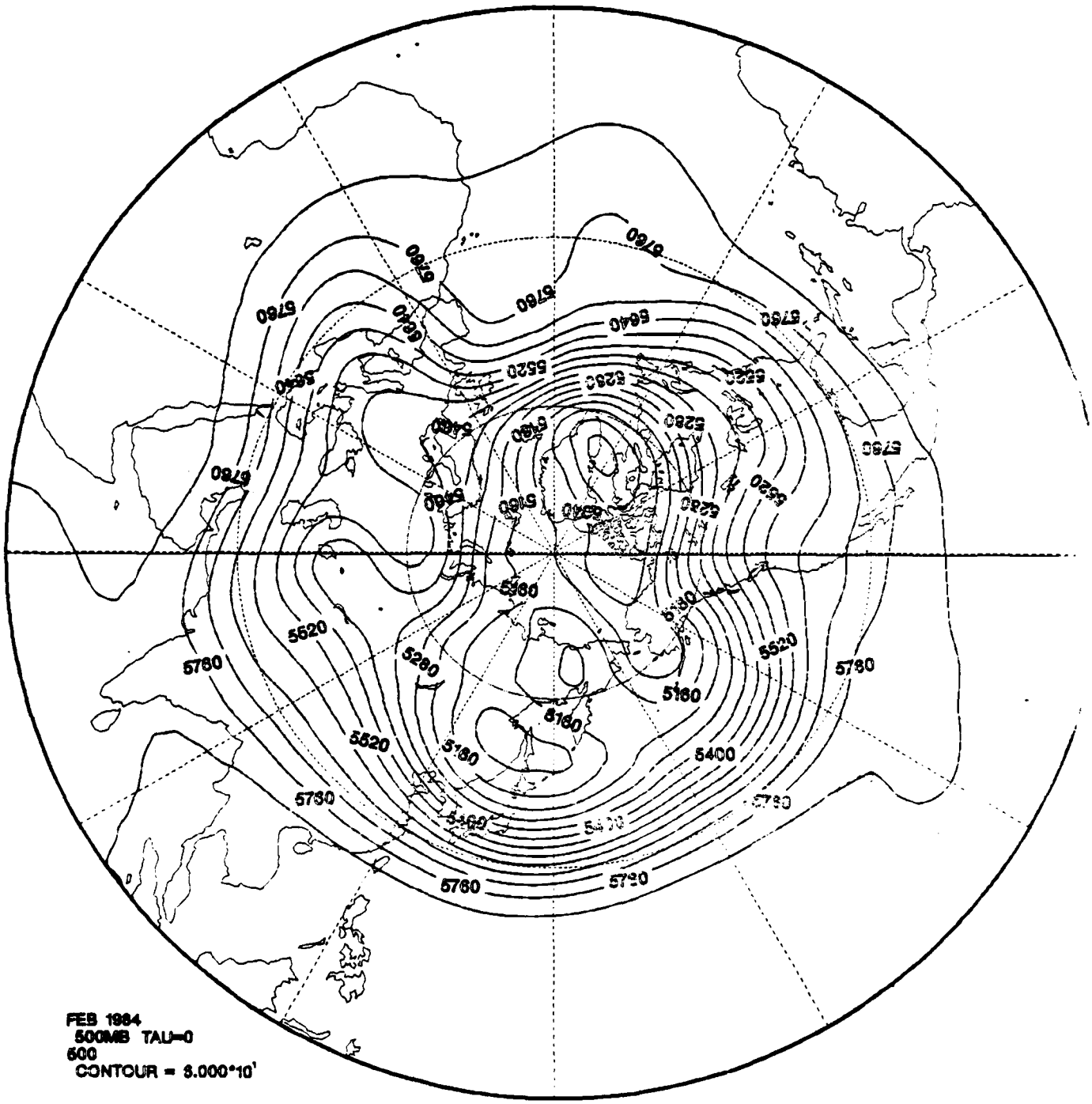

22A As in Fig. 1A but for Feb 1984. Contour interval is 60 m.

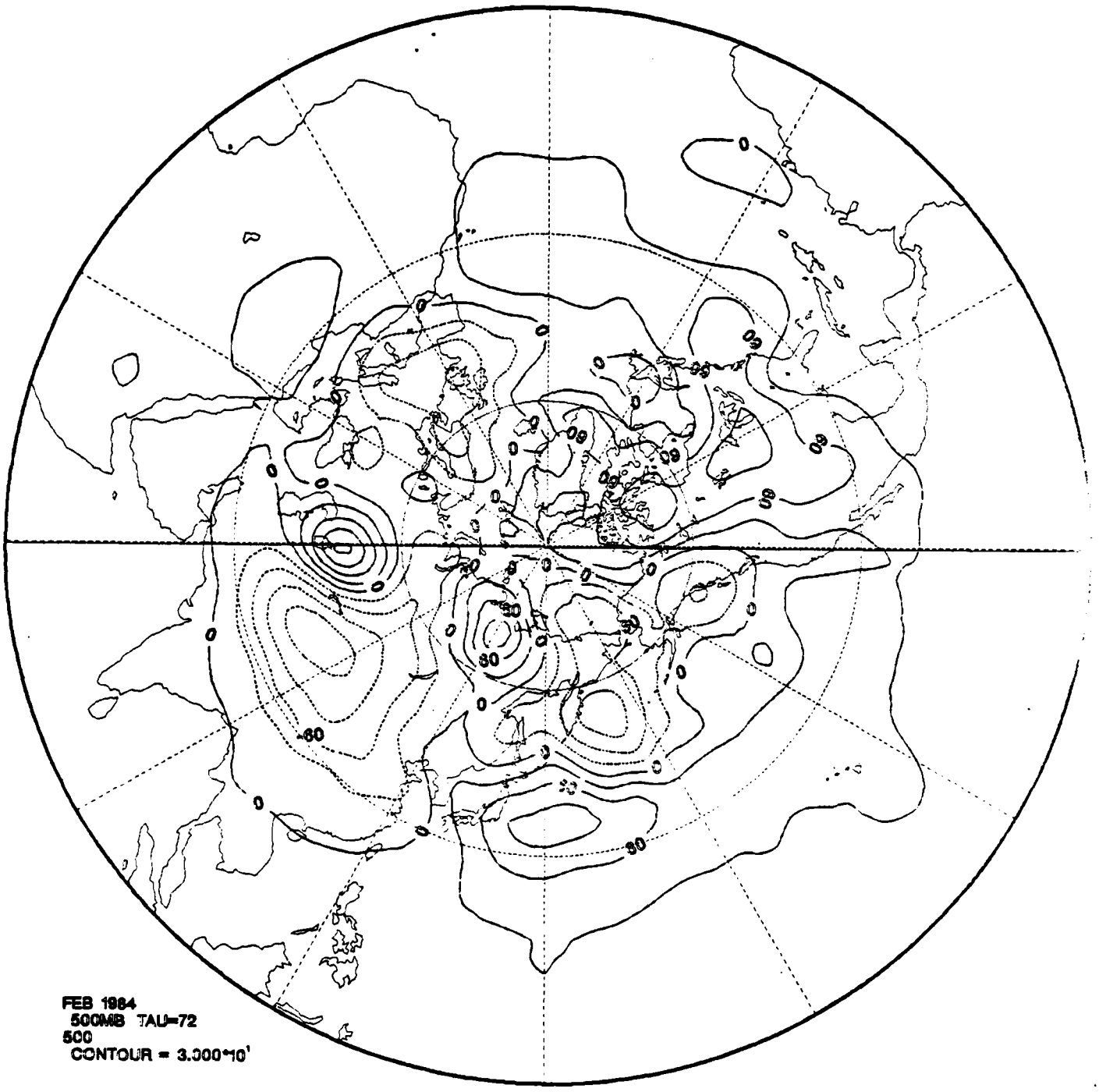

22B As in Fig. 1C but for Feb 1984. Contour interval is 30 m.

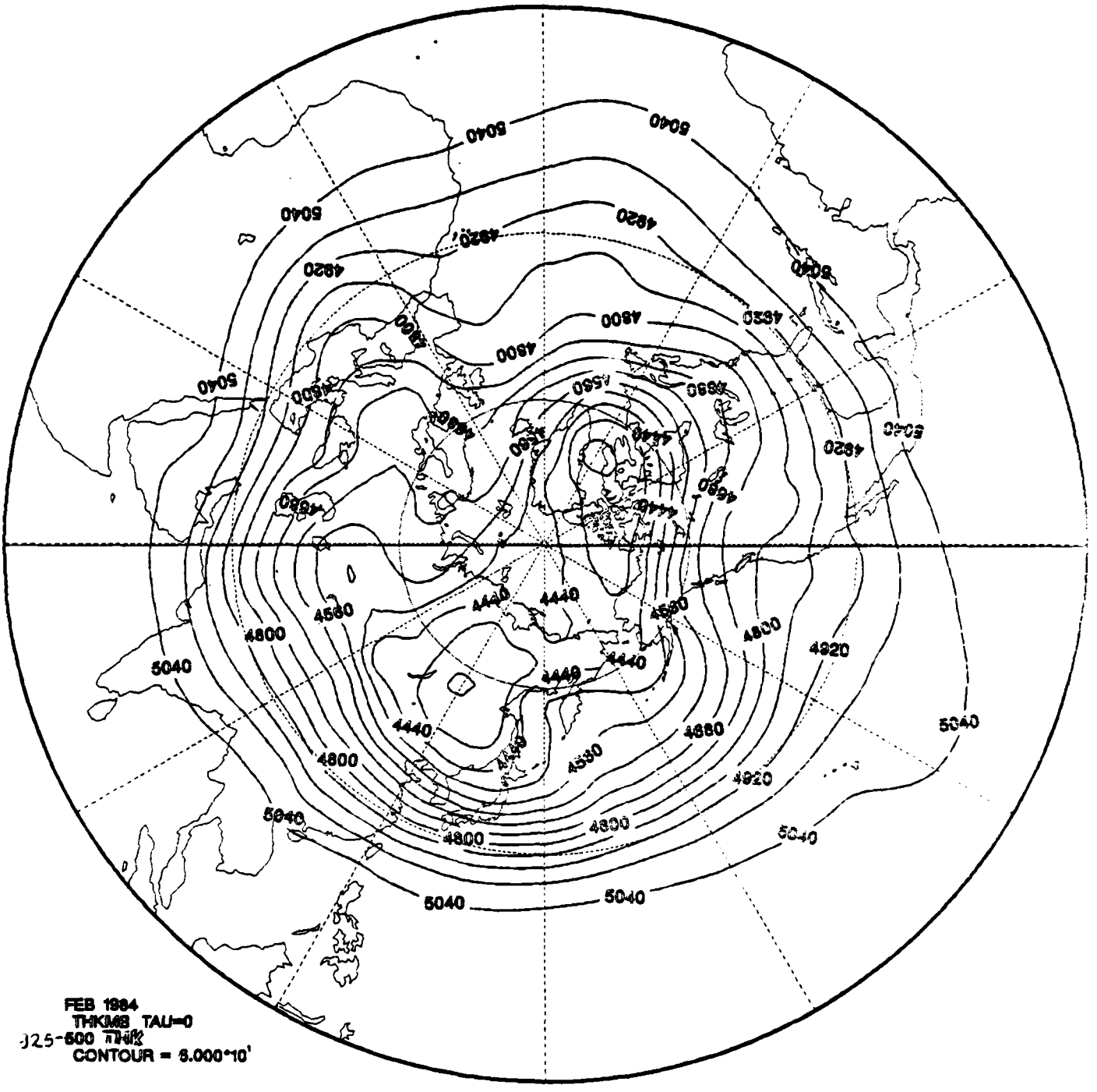

23A As in Fig. 2A but for Feb 1984. Contour interval is 60 m.

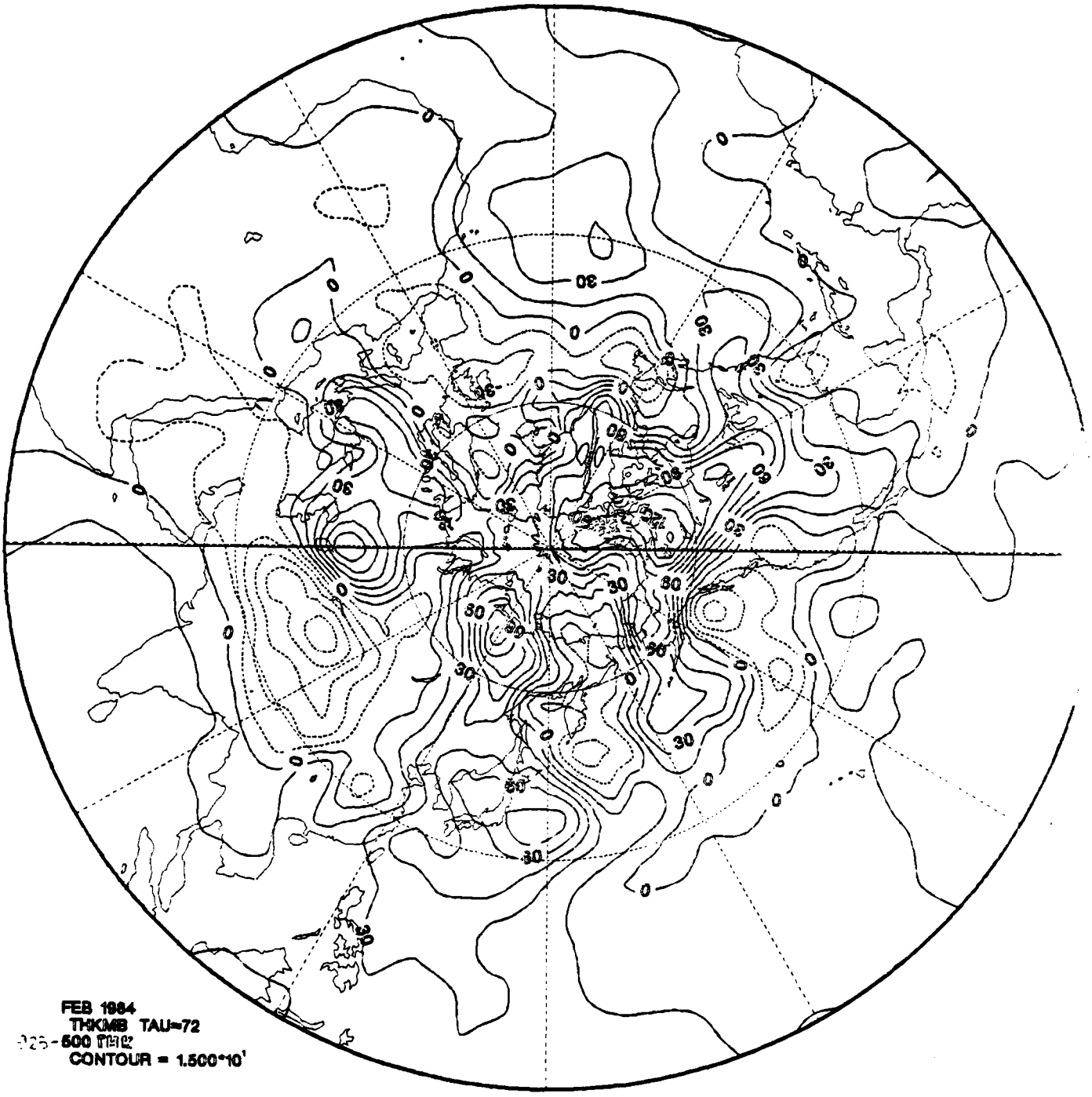

23B As in Fig. 2B but for Feb 1984. Contour interval is 15 m.

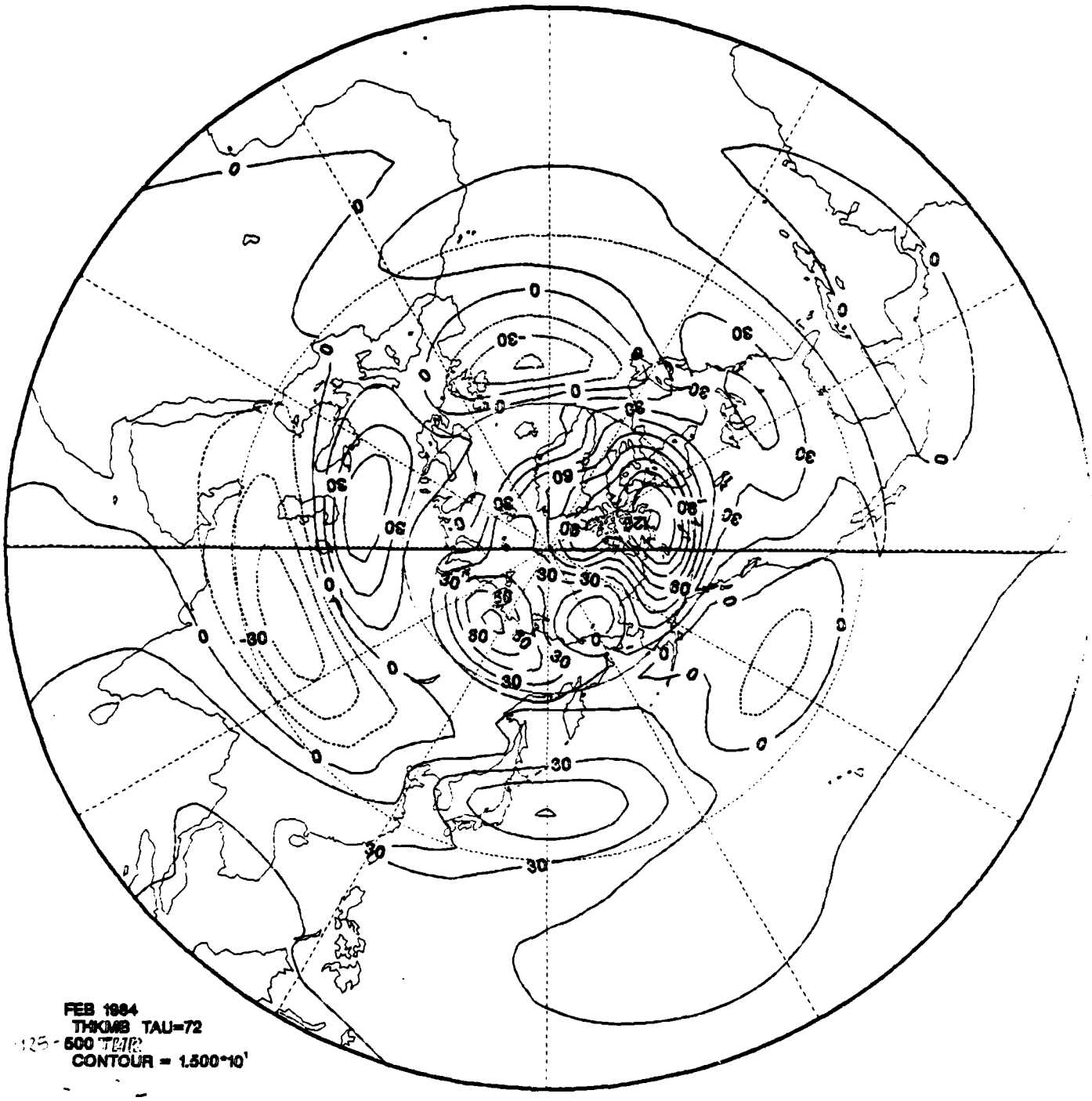

23C As in Fig. 2C but for Feb 1984. Contour interval is 3 dm.

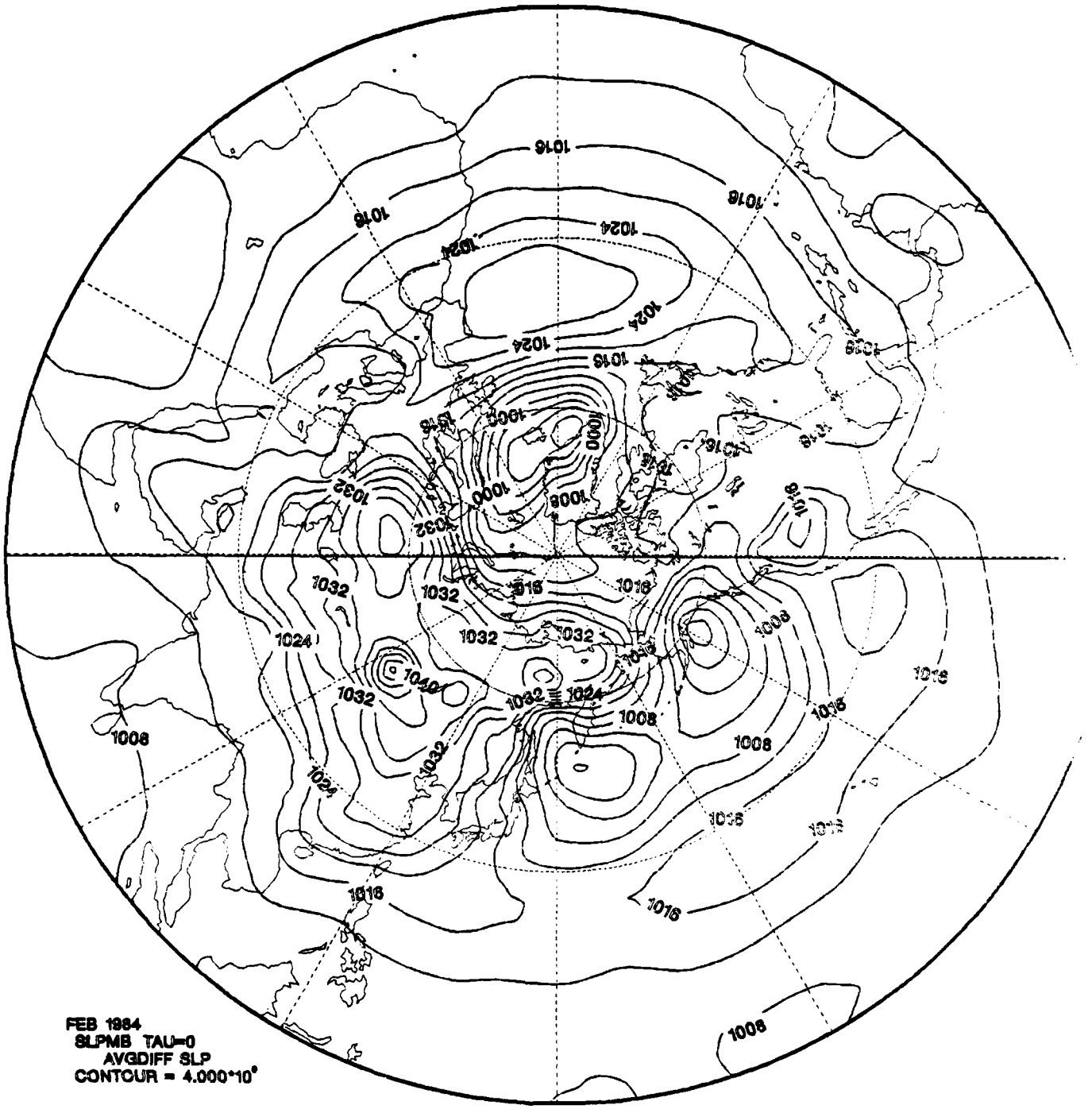

24A As in Fig. 3A but for Feb 1984. Contour interval [illegible] mb.

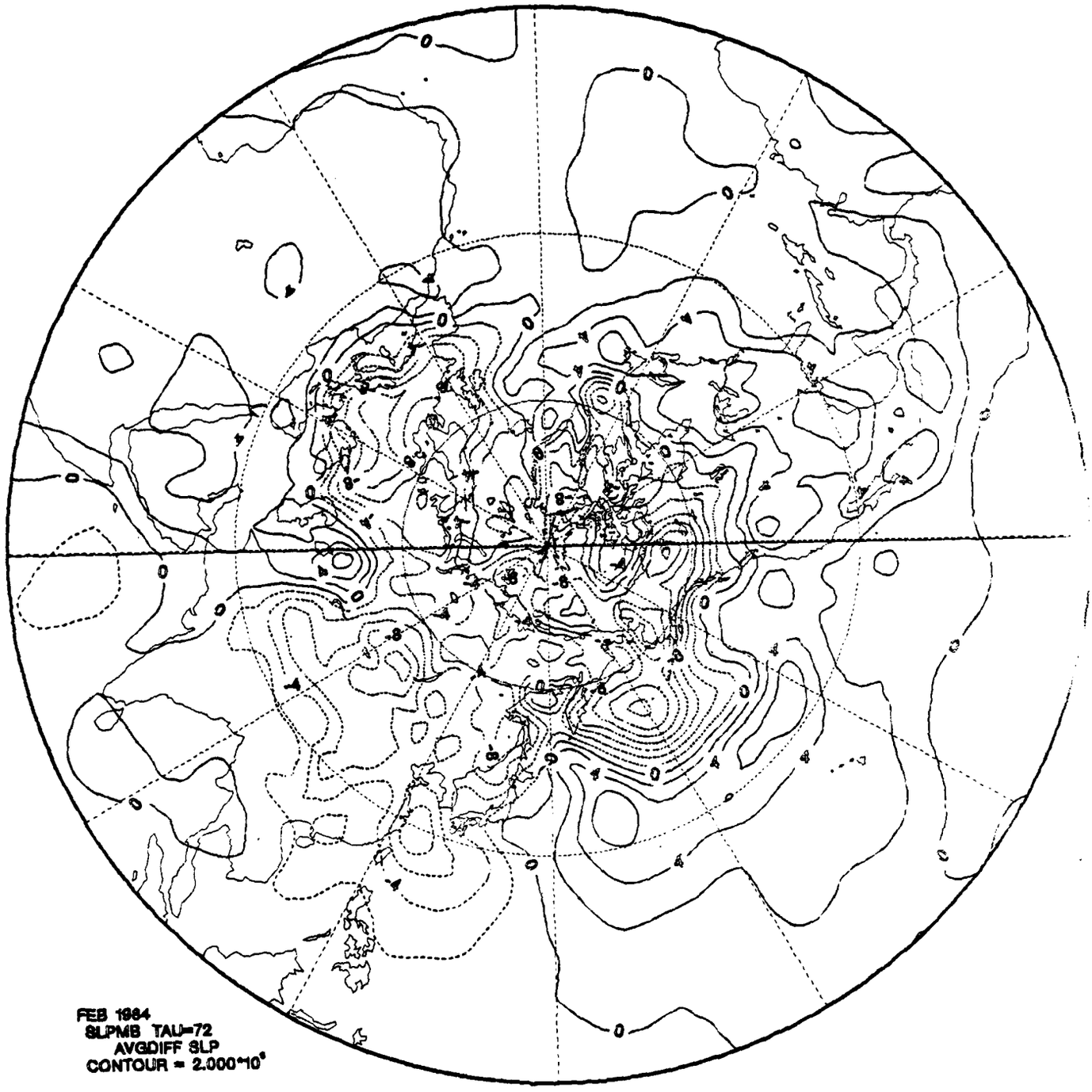

Fig. 43 As in Fig. 38 but for Feb 1984. Contour interval is 2 mb.

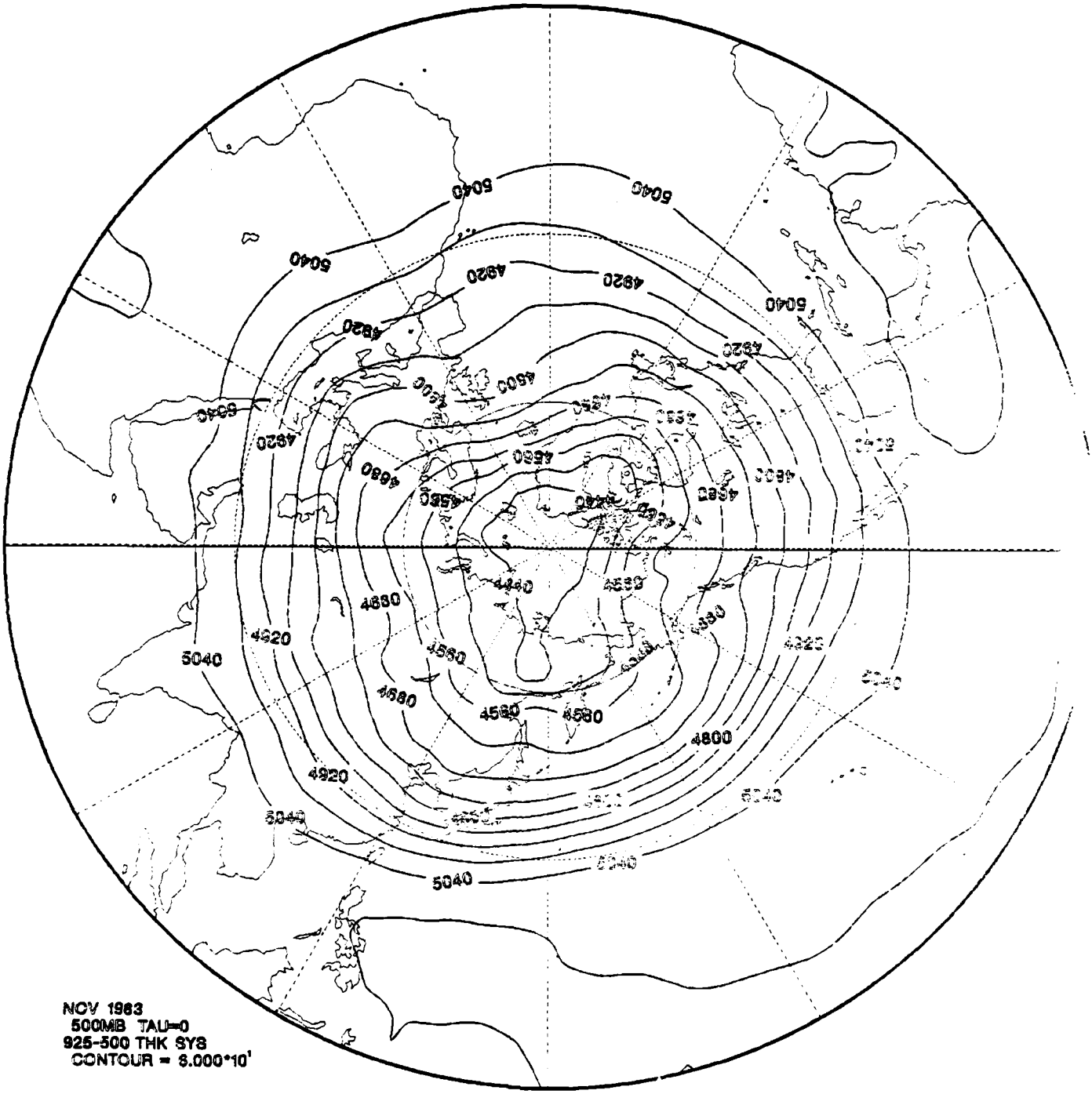

25A ... as in Fig. 2A but for Nov 1963. Contour interval is 8...

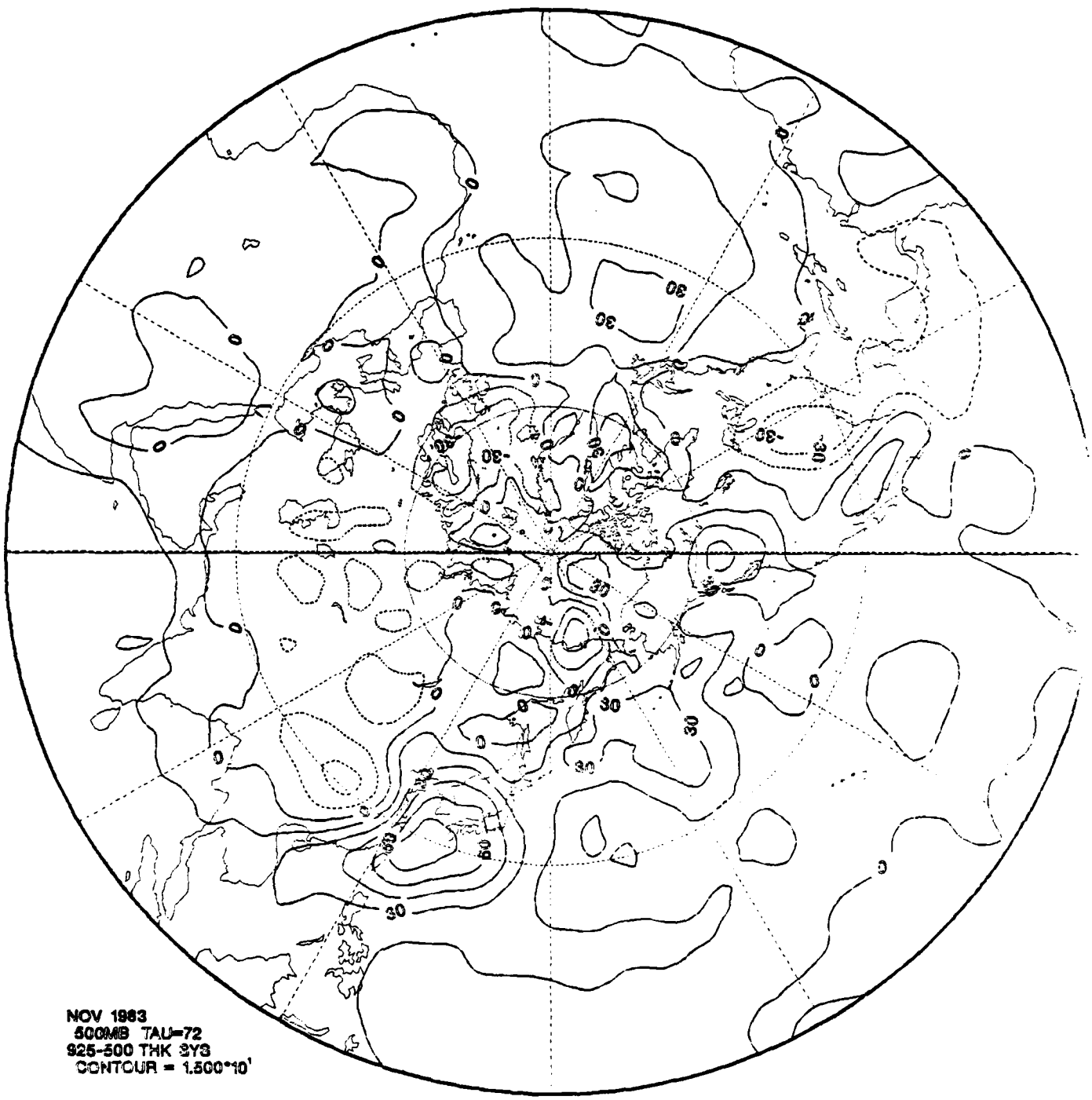

25B As in Fig. 2B but for Nov 1983. Contour interval [illegible] m.

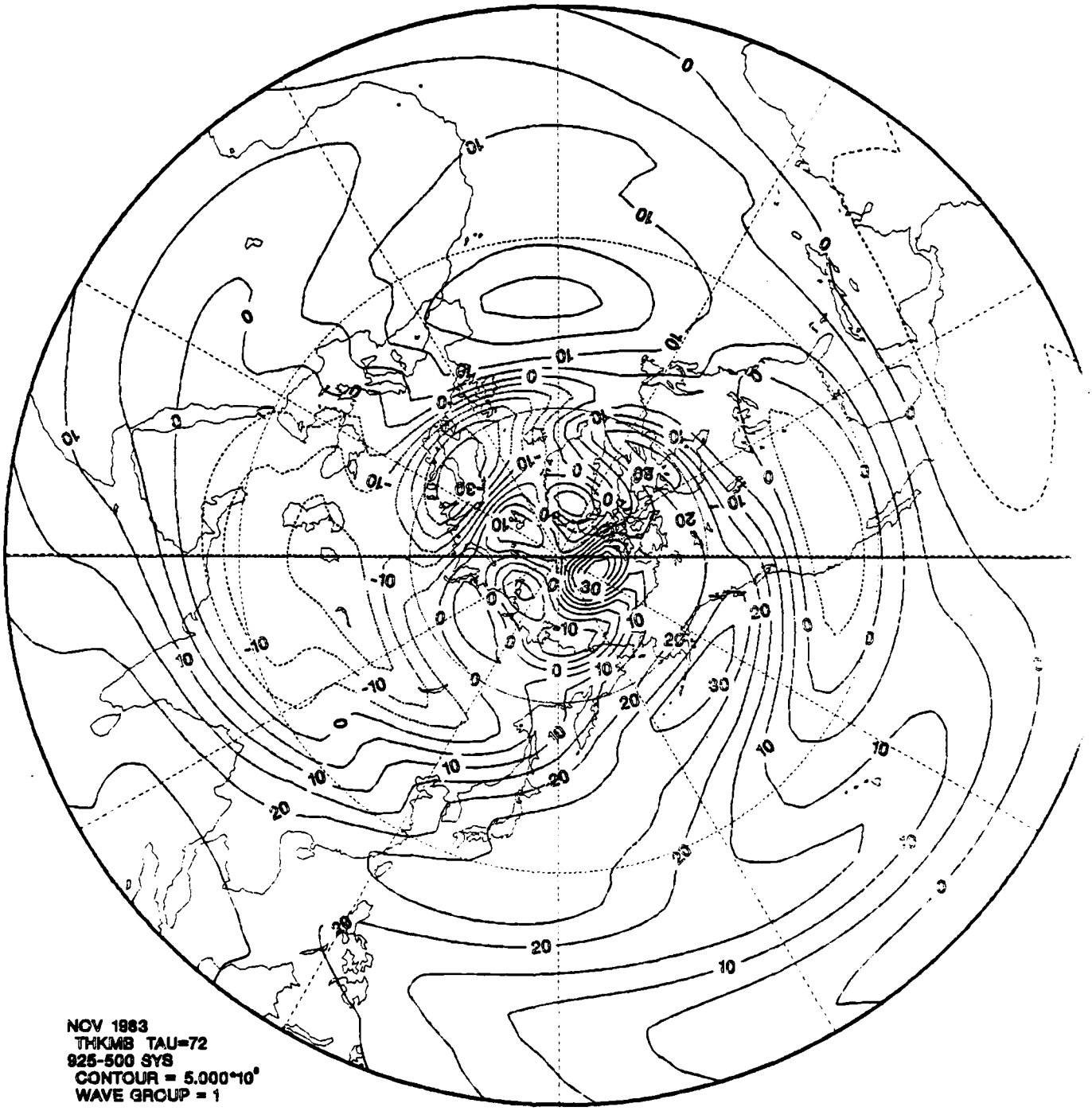

25C As in Fig. 2C but for Nov 1983. Contour interval is 5 m.

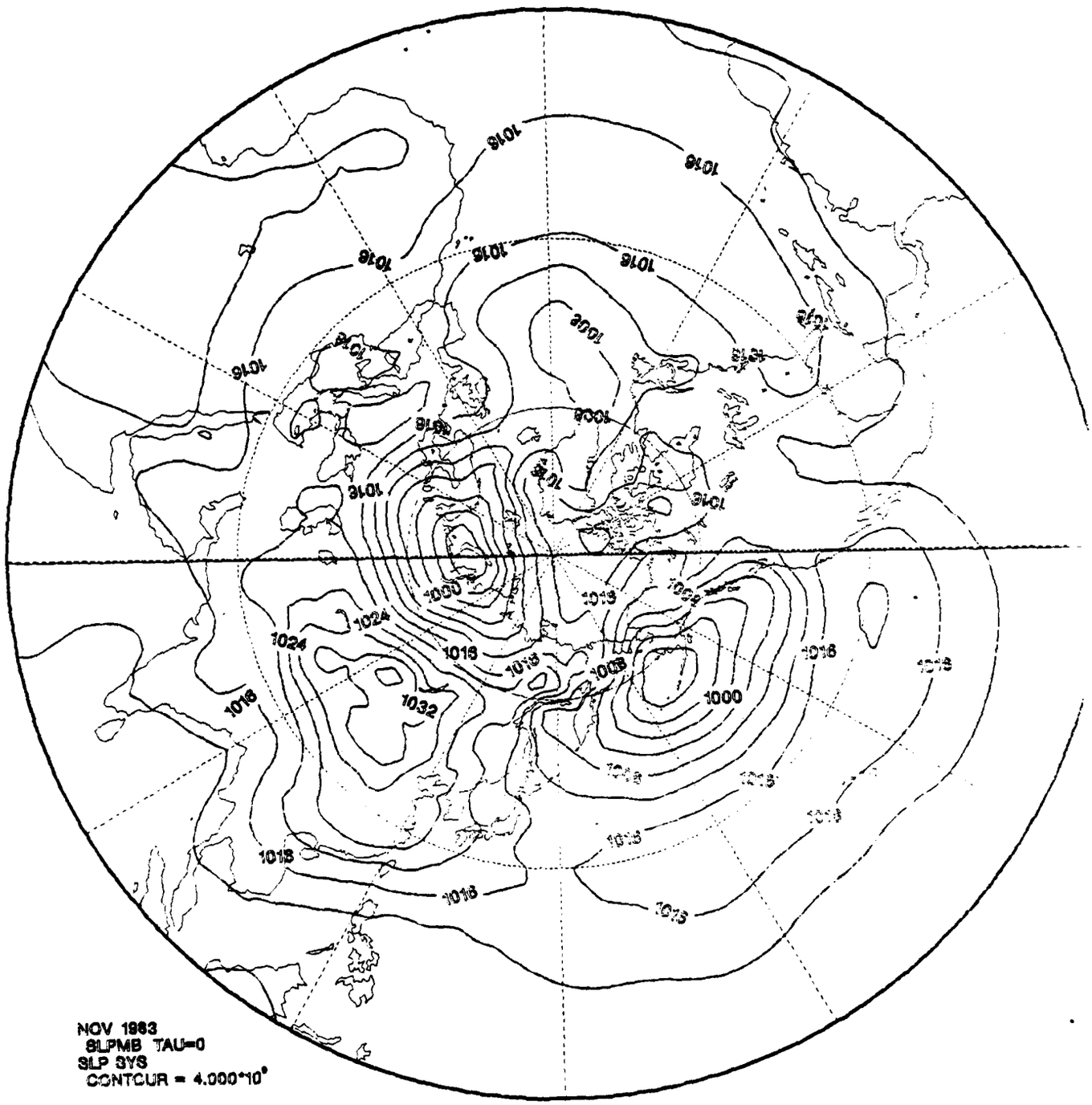

26A As in Fig. 3A but for Nov 1983. Contour interval is 4 mb.

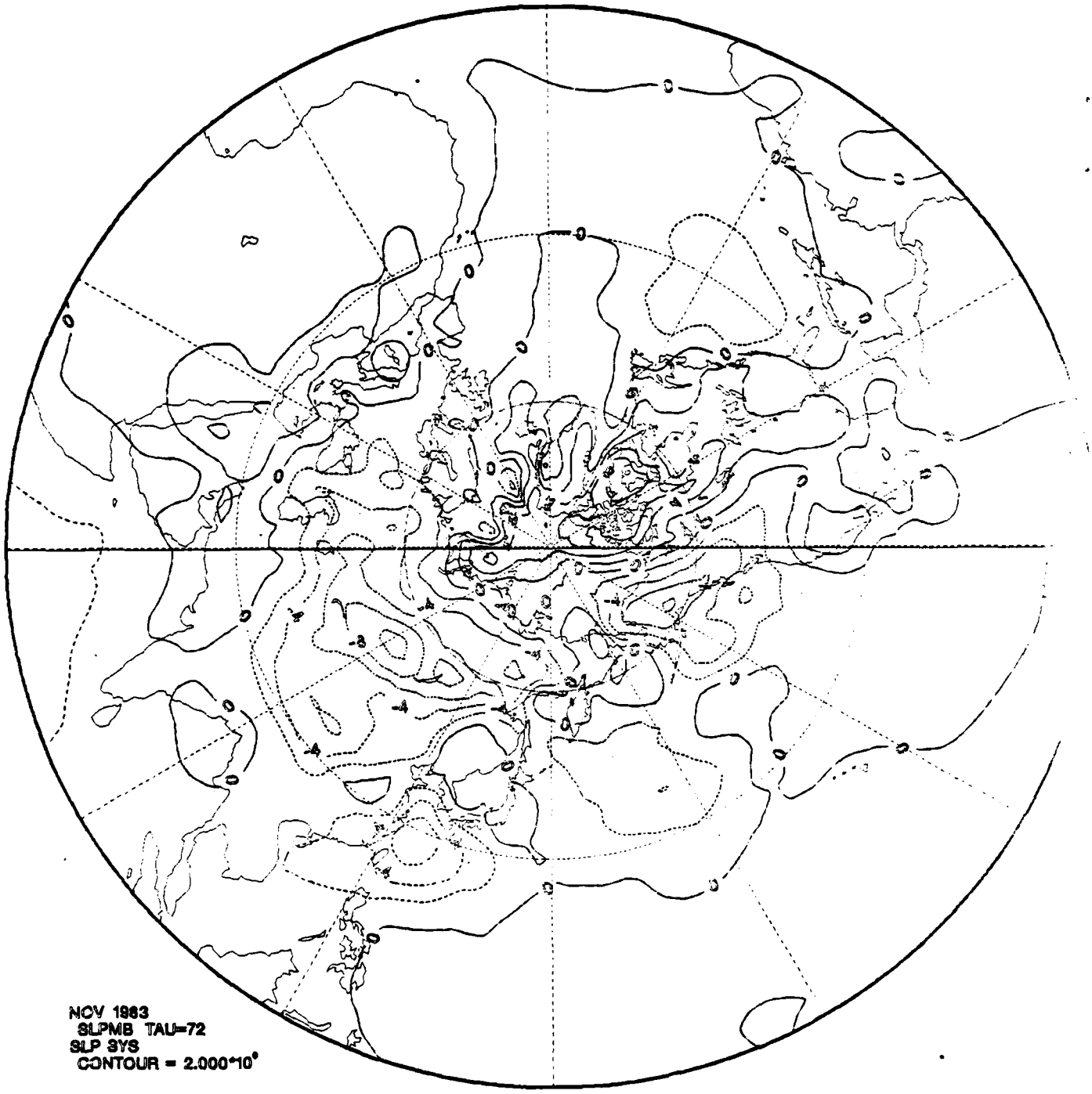

26B As in Fig. 3B but for Nov 1983. Contour interval is 2 mb.

INITIAL DISTRIBUTION LIST

		No. Copies
1.	Defense Technical Information Center Cameron Station Alexandria, Virginia 22314	2
2.	Library, Code 0142 Naval Postgraduate School Monterey, California 93943	2
3.	Department of Meteorology Library Code 63, Naval Postgraduate School Monterey, California 93943	1
4.	Prof. James S. Boyle, Code 63Xj Naval Postgraduate School Monterey, California 93943	2
5.	Prof. C. H. Wash, Code 63Wx Naval Postgraduate School Monterey, California 93943	30
6.	Commander Naval Oceanography Command NSTL Station Bay St. Louis, MS 39529	1
7.	Commanding Officer Naval Oceanographic Office NSTL Station Bay St. Louis, MS 39529	1
8.	Commanding Officer Naval Ocean Research and Development Activity NSTL Station Bay St. Louis, MS 39529	1
9.	Commanding Officer Naval Environmental Prediction Monterey, CA 93940	1
10.	Chairman, Oceanography Department U.S. Naval Academy Annapolis, MD 21402	1
11.	Office of Naval Research (Code 480) Naval Ocean Research and Development Activity NSTL Station Bay St. Louis, MS 39529	1
12.	Prof. R. J. Renard, Code 63Rd Naval Postgraduate School Monterey, California 93943	1

13. Research Administration Office 1
Code 012
Naval Postgraduate School
Monterey, CA 93943

END

FILMED

3-86

DTIC